2001

# Modeling the response of top-down control exerted by gelatinous carnivores on the Black Sea pelagic food web

Temel Oguz
*Institute of Marine Sciences, Middle East Technical University*

Hugh W. Ducklow
*Virginia Institute of Marine Science*

Jennifer E. Purcell
*University of Maryland*

Paola Malanotte-Rizzoli
*Massachusetts Institute of Technology*

JOURNAL OF GEOPHYSICAL RESEARCH, VOL. 106, NO. C3, PAGES 4543–4564, MARCH 15, 2001

# Modeling the response of top-down control exerted by gelatinous carnivores on the Black Sea pelagic food web

Temel Oguz,[1] Hugh W. Ducklow,[2] Jennifer E. Purcell,[3]
and Paola Malanotte-Rizzoli,[4]

**Abstract.** Recent changes in structure and functioning of the interior Black Sea ecosystem are studied by a series of simulations using a one-dimensional, vertically resolved, coupled physical-biochemical model. The simulations are intended to provide a better understanding of how the pelagic food web structure responds to increasing grazing pressure by gelatinous carnivores (medusae *Aurelia aurita* and ctenophore *Mnemiopsis leidyi*) during the past 2 decades. The model is first shown to represent typical eutrophic ecosystem conditions of the late 1970s and early 1980s. This simulation reproduces reasonably well the observed planktonic food web structure at a particular location of the Black Sea for which a year-long data set is available from 1978. Additional simulations are performed to explore the role of the *Mnemiopsis*-dominated ecosystem in the late 1980s. They are also validated by extended observations from specific years. The results indicate that the population outbreaks of the gelatinous species, either *Aurelia* or *Mnemiopsis*, reduce mesozooplankton grazing and lead to increased phytoplankton blooms as observed throughout the 1980s and 1990s in the Black Sea. The peaks of phytoplankton, mesozooplankton, *Noctiluca*, and gelatinous predator biomass distributions march sequentially as a result of prey-predator interactions. The late winter diatom bloom and a subsequent increase in mesozooplankton stocks are robust features common to all simulations. The autotrophs and heterotrophs, however, have different responses during the rest of the year, depending on the nature of grazing pressure exerted by the gelatinous predators. In the presence of *Mnemiopsis*, phytoplankton have additional distinct and pronounced bloom episodes during the spring and summer seasons. These events appear with a 2 month time shift in the ecosystem prior to introduction of *Mnemiopsis*.

## 1. Introduction

In a celebrated paper, *Hairston et al.* [1960] (hereinafter referred to as HSS) predicted that effects of top predators could cascade across multiple trophic levels and on down the food chain to regulate producer populations at the base of the trophic pyramid. The relative strength of bottom-up (resource availability) versus top-down (predator) controls on ecosystem structure and dynamics is still a hotly debated topic in ecology [*Carpenter et al.*, 1985]. The existence of trophic cascades has been largely confined to freshwater aquatic communities [*Strong*, 1992], with fewer examples from marine and terrestrial systems (although HSS based their arguments on terrestrial communities). *Micheli* [1999] suggested that cascades were attenuated in marine systems by incomplete coupling among trophic levels. The exceptions to the absence of trophic cascades in the marine environment seem to involve gelatinous predators [*Verity and Smetacek*, 1996]. Introduction of the ctenophore *Mnemiopsis leidyi* into the Black Sea in ballast water from the east coast of North America in the middle-to-late 1980s represents a clear example of the imposition of a new form of top-down (predator) control on the Black Sea ecosystem already severely impacted by eutrophication [*Zaitsev and Mamaev*, 1997]. In this paper we utilize a one-dimensional physical-biological ecosystem model of the Black Sea to explore population

[1]Institute of Marine Sciences, Middle East Technical University, Erdemli, Icel, Turkey.
[2]Virginia Institute of Marine Sciences, College of William and Mary, Gloucester Point, Virginia.
[3]Center for Environmental Science, Horn Point Environmental Laboratory, University of Maryland, Cambridge, Maryland.
[4]Department of Earth, Atmospheric and Planetary Sciences, Massachusetts Institute of Technology, Cambridge, Massachusetts.



Paper number 1999JC000078.
0148-0227/01/1999JC000078$09.00

dynamics prior to and following *Mnemiopsis* introduction into the system.

### 1.1. General Ecosystem Characteristics

The Black Sea, with one of the largest enclosed catchment basins in the world, receives extraordinarily high nutrient loading and contaminants from rivers draining half of Europe and parts of Asia [*Mee*, 1992]. Its past 2 decades are identified as a nonequilibrium ecosystem, in transition to its present low-biodiversity eutrophic state. The new ecosystem is characterized by profound differences in the variability, size, and taxonomic structure of the phytoplankton community, with population outbreaks of the opportunistic species *Noctiluca scintillans* and the gelatinous predators *Aurelia aurita*, and *Mnemiopsis leidyi*, hereinafter referred to by genus.

Before the 1970s, diatoms were the dominant phytoplankton group with their maximum stocks in the late winter to early spring [*Mikaelyan*, 1997]. After the 1970s, summer blooms of dinoflagellates became a major signature of the ecosystem [*Mikaelyan*, 1997; *Moncheva and Krastev*, 1997]. The zooplankton community was characterized by major increases in the *Aurelia* and *Pleurobrachia pileus* (another gelatinous predator) populations during the late 1970s and the early 1980s and in the *Mnemiopsis* population toward the end of the 1980s [*Shushkina et al.*, 1998; *Kovalev et al.*, 1998; *Shiganova et al.*, 1998; *Kideys et al.*, 2000]. Order of magnitude increases in abundance of the jellyfish *Aurelia* and the omnivorous dinoflagellate *Noctiluca* during the late 1970s were, in fact, the first alarming signal of the profound ecosystem changes occurring in the Black Sea. The sudden increase in the *Mnemiopsis* population caused further reduction in the biomass of the mesozooplankton community as well as in fish eggs and larvae during the late 1980s [*Shushkina et al.*, 1998]. These effects, together with overfishing, ultimately caused a collapse of commercial fish stocks (anchovy, sprat, and horse mackerel) during the early 1990s [*Rass*, 1992]. As compared with the other groups, little information is available on potential changes in the microbial community. Details on Black Sea ecosystem characteristics are documented by *Zaitsev and Mamaev* [1997], *Ozsoy and Mikaelyan* [1997] and *Ivanov and Oguz* [1998a, 1986b].

### 1.2. Feeding, Life History, Interannual and Seasonal Variations in *Aurelia* and *Mnemiopsis* Stocks

The predominant gelatinous species in the Black Sea since the 1970s, the jellyfish *Aurelia* and the ctenophore *Mnemiopsis*, have been shown to be important predators of zooplankton and ichthyoplankton [*Zaitsev and Mamaev*, 1997]. Similarly, *Aurelia* in the Kiel Bight, Germany, when abundant, was shown to reduce zooplankton standing stocks and to alter plankton species composition [*Schneider and Behrends*, 1989; *Behrends and Schneider*, 1995]. High abundance of *Aurelia* was correlated with low numbers of herring larvae there [*Moller*, 1984]. Low mesozooplankton densities frequently have been found during periods of high *Mnemiopsis* densities [*Purcell*, 1988; *Shiganova*, 1998], and they are voracious consumers of zooplankton [e.g., *Kremer*, 1976b; *Purcell et al.*, 1994b]. *Mnemiopsis* also consumed ichthyoplankton, especially fish eggs, removing as much as 39% during the 20 hour egg stage in Chesapeake Bay [*Purcell et al.*, 1994a]. The potential effects of medusae and ctenophores on zooplanktivorous fish populations, such as anchovies, would be due to both direct predation on the young stages and potential competition for food with all life stages.

*Aurelia* and *Mnemiopsis* have markedly different life histories that greatly affect their population dynamics. Production of *Aurelia* medusae is highly seasonal. *Aurelia* has a perennial benthic polyp stage that buds small (1-2 mm) medusae, which begin rapid growth when food is abundant in the spring [e.g., *Hamner and Jenssen*, 1974; *Moller*, 1980; *Lucas and Williams*, 1994; *Schneider and Behrends*, 1989]. Large populations of the sexually reproducing dioecious medusae are usually reached and maintained in summer. Fertilized eggs of *Aurelia* are brooded on the females, and when released, the larvae settle on hard substrates to become polyps. Medusae abundance and biomass decrease rapidly in late summer or fall. The causes of this seasonal mass mortality among medusae are poorly documented but may include predation [*Purcell*, 1991; *Mills*, 1993], destruction by hyperiid amphipods and senescence [*Mills*, 1993], low food abundance, and possible sensitivity to colder temperatures. The next generation of medusae arises from the annual budding of the polyps.

By contrast, *Mnemiopsis* ctenophores are holoplanktonic and hermaphroditic. Egg production, and resulting population size, is dependent upon the amount of planktonic foods available [*Reeve et al.*, 1992]. Development is direct. Predation by scyphomedusae can limit *Mnemiopsis* populations during the summer in Chesapeake Bay [*Purcell and Cowan*, 1995]. Populations in environments with cold winters decrease in the fall [*Kremer*, 1994] partly because of predation by *Beroe* ctenophores [*Kremer*, 1976b], destruction by parasitic anemone larvae [*Bumann and Puls*, 1996], low food abundance, and possible sensitivity to cold and turbulent conditions. *Mnemiopsis* populations are seeded from survivors when conditions improve. Where winters are mild, *Mnemiopsis* can be present all year (reviewed by *Kremer* [1994]).

Our knowledge of the interannual and seasonal biomass variations of *Aurelia* and *Mnemiopsis* in the Black Sea comes from a set of data based on field work performed during the past 20 years by the Shirshov Institute of Oceanology, Moscow, the Institute of Biology of Southern Seas, Sevastopol, and the Institite of Marine Sciences, Erdemli [*Shushkina and Musayeva*, 1983, 1990; *Lebedeva and Shushkina*, 1991, 1994; *Vinogradov*

**Table 1.** Interannual and Seasonal Variations of *Aurelia* and *Mnemiopsis* biomass Within the Interior Part of the Black Sea [a]

| Year | Month | *Aurelia*, g C $m^{-2}$ | *Mnemiopsis*, g C $m^{-2}$ |
|---|---|---|---|
| 1978 | 10 | 3.52 | - |
| 1984 | 4 | 3.41 | - |
| | 5 | 3.89 | - |
| 1985 | 10 | 1.83 | - |
| 1986 | 6 | 0.56 | - |
| 1991 | 2 | 0.98 | 0.57 |
| | 3 | 1.66 | 0.84 |
| | 4 | 1.18 | 0.79 |
| | 6 | 0.26 | 0.13 |
| 1992 | 8 | 0.79 | 0.19 |
| 1993 | 4 | 0.44 | 0.02 |
| | 8 | 0.67 | 0.22 |
| 1994 | 2 | 0.25 | 0.29 |
| | 4 | 1.18 | 0.26 |
| 1995 | 3 | 0.86 | 0.49 |
| 1996 | 4 | 0.20 | 0.28 |
| | 6 | 0.40 | 0.14 |
| 1997 | 7 | 0.44 | 0.12 |

[a]Data are provided by A. E. Kideys.

*and Shushkina*, 1992; *Mutlu et al.*, 1994; *Khoroshilov*, 1994; *Finenko et al.*, 1995; *Minkina and Pavlova*, 1995; *Vinogradov et al.*, 1996; *Shiganova*, 1998; *Kovalev et al.*, 1998; *Mutlu*, 1999; *Kideys et al.*, 2000]. Most of those data typically were reported in terms of wet weight, which we converted to carbon weight using factors of 0.002 for *Aurelia* and 0.001 for *Mnemiopsis*. These conversions are similar to those measured earlier for *Aurelia* (e.g., 0.003 by *Shushkina and Vinogradov* [1991], and 0.0016 by *Larson* [1986]) and for *Mnemiopsis* (e.g., 0.0006 by *Kremer* [1976a], 0.0007 by *Shushkina and Vinogradov* [1991], and 0.0005 by *Nemazie et al.* [1993]).

The data presented in Table 1 involving different sets of measurements from 1978 to 1997 suggest three stages in changes of *Mnemiopsis* and *Aurelia* in the Black Sea. Starting from the middle 1970s, the period up to 1987 represents a pre-*Mnemiopsis* era dominated by *Aurelia* medusae. *Aurelia* biomass exhibited two seasonal peaks of about 2-3 gC $m^{-2}$ during May and October and attained minimum levels during the summer and winter seasons (Figure 1). The summertime reduction in the *Aurelia* biomass is marked clearly and consistently by the data listed in Table 1. *Aurelia* populations in other locations also have decreased in biomass in summer [*Hamner and Jenssen*, 1974; *Van der Veer and Oorthuysen*, 1985; *Lucas and Williams*, 1994; *Ishii and Bamstedt*, 1998]. However, autumn rebounds in those populations were not seen. The biomass of *Aurelia* has shown two peaks in some locations in some years [*Olesen et al.*, 1994; *Schneider and Behrends*, 1989]. The biomass of *Aurelia* in other locations declines in the autumn [*Moller*, 1980; *Olesen et al.*, 1994; *Schneider and Behrends*, 1989]. The summer reduction in the Black Sea seems to be related to food competition as both *Aurelia* and small pelagic fishes (such as anchovy and horse mackerel) feed on the same trophic levels, and the abundance of competing small pelagic fishes are maximal during the summer period [*Gucu*, 1997].

The years 1989 and 1990, in contrast, constitute a second period in which *Aurelia* blooms were practically replaced by those of *Mnemiopsis* (Figure 1). The *Aurelia* biomass remained <1 gC $m^{-2}$ throughout the year during this period. The *Mnemiopsis* biomass, in contrast, which was never at measurable quantities before (see Table 1), reached about 1.0 gC $m^{-2}$ in August 1988. During 1989, the first *Mnemiopsis* peak of the year was about 2.0 gC $m^{-2}$ during February-March. This peak

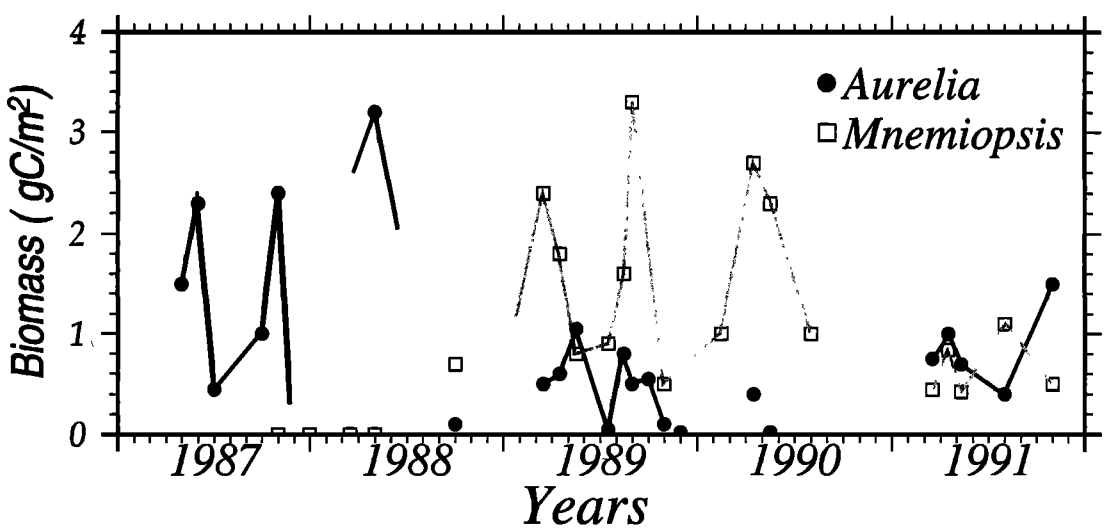


**Figure 1.** Variations of *Aurelia* and *Mnemiopsis* biomass (in gC $m^2$) during the years 1987-1991. Each data point represents an average of measurements carried out within the interior basin [after *Shushkina et al.*, 1998].

was followed by a decreasing trend in biomass in June-July and, later, by a second peak of about 3.0 gC $m^{-2}$ during August-September. The next set of measurements, performed during late winter to early spring 1990, also recorded a strong *Mnemiopsis* peak of the order of 3.0 gC $m^{-2}$, whereas the *Aurelia* biomass remained only around 0.5 gC $m^{-2}$. *Mnemiopsis* biomass again decreased in the late spring to summer period. *Mnemiopsis* populations along the eastern coast of the United States show from one summertime peak in the north to multiple peaks in the south (reviewed by *Kremer* [1994] and *Purcell et al.* [1994b]).

The period after 1991 represents a third stage in the ecosystem transformation in which *Mnemiopsis* and *Aurelia* tended to have almost equal stocks in the Black Sea food web. According to the composite data given in Table 1 for the period of 1991-1997 [see also *Kovalev et al.*, 1998], they seemed to attain a new equilibrium state in which neither dominated the food web. They both had comparable peak biomass values of about 1.0-1.5 gC $m^{-2}$. Thus the 1989-1991 period may represent a transition state following *Mnemiopsis* invasion in the late 1980s.

### 1.3. Existing Modeling Studies

There have been some attempts to model pelagic food web structure in the Black Sea using externally specified yearly cycles of the mixed layer depth and temperature from the available climatological data [*Lebedeva and Shushkina*, 1994; *Eeckhout and Lancelot*, 1997; *Cokasar and Ozsoy*, 1998]. *Lebedeva and Shushkina* [1994] explored ecosystem characteristics before and after the introduction of *Mnemiopsis* using a pelagic lower trophic food web structure comprising phytoplankton, bacteria, protozoa, mesozooplankton, *Aurelia* and *Mnemiopsis*, particulate and dissolved organic matter, and nutrient compartments. Through application of different variants of the *Fasham et al.* [1990] model to dynamically different regions of the Black Sea, *Cokasar and Ozsoy* [1998] presented a series of simulations to explore factors responsible for the observed regional differences in productivity. *Eeckhout and Lancelot* [1997] provided a brief account of their preliminary modeling of the role of nutrient enrichment for destabilization of the northwestern shelf ecosystem. None of these exercises, however, offered a comprehensive view of the response of the top-down control exerted by gelatinous predators on the Black Sea pelagic food web.

The structure and functioning of the plankton community, coupled with biogeochemical processes taking place within the deeper parts of the upper layer water column of the interior Black Sea are studied by means of vertically resolved coupled physical-biological models [*Oguz et al.*, 1996, 1998a, 1999, 2000]. An overview of some of these efforts and important findings are presented by *Oguz et al.* [1998b]. A simplified five compartment version with single groups of phytoplankton and zooplankton, plus detritus, ammonium, and nitrate, was developed by *Oguz et al.* [1996]. It was also used by *Staneva et al.* [1998] for studying the response to different meteorological conditions on the upper layer physical-biological structures. A slightly more complex form of the model with two classes of phytoplankton (diatoms and flagellates) and two zooplankton size groups (microzooplankton and mesozooplankton) was introduced later by *Oguz et al.* [1999]. These efforts concentrated mainly on simulation of annual primary production characteristics rather than focusing on food web dynamics. *Oguz et al.* [1998a] elaborate the model further by including an additional zooplankton compartment representing an aggregated group of gelatinous carnivores in the food web, as well as a simplified representation of the microbial loop involving bacterial dynamics and dissolved organic matter production. This model was further extended to provide a unified representation of the dynamically coupled oxic-suboxic-anoxic system [*Oguz et al.*, 2000]. The coupled northwestern shelf-deep basin ecosystem structure was investigated with a three-dimensional food web model of comparable complexity by *Gregoire et al.* [1998].

### 1.4. Aim and Scope of the Present Work

In the present work we use a slightly modified version of the process model described by *Oguz et al.* [1998a] to explore the nature of the trophic interactions between the components of the ecosystem at two different stages during the past 2 decades. A series of numerical simulation experiments was designed to study the response of different grazing pressures exerted by gelatinous carnivores on the overall annual plankton structure within interior Black Sea waters. Our particular objective is to complement our limited observational knowledge with the model findings and then reach a quantitative understanding of the functioning of the Black Sea ecosystem in terms of interactions among different groups of the food web. In section 2 we describe model formulation involving governing equations on predator-prey dynamics among phytoplankton and zooplankton, as well as the boundary, initial conditions, and numerical procedure. We then show how the procedure can successfully reproduce the annual cycle of plankton structure obtained by biweekly observations at a particular station off the Caucasian coast during 1978 (section 3). This experiment defines the eutrophied ecosystem conditions prior to the introduction of *Mnemiopsis*. In section 4 we provide additional simulations for representing the state of the ecosystem after the introduction of *Mnemiopsis*. In section 5, we give a summary of results and conclusions. Further details on formulation of other water column processes and biogeochemical cycling, not included in section 2, are given in the Appendix A.

## 2. Model Formulation

### 2.1. Description of Model Structure

The pelagic planktonic food web combined with particulate matter decomposition and nitrogen cycling in

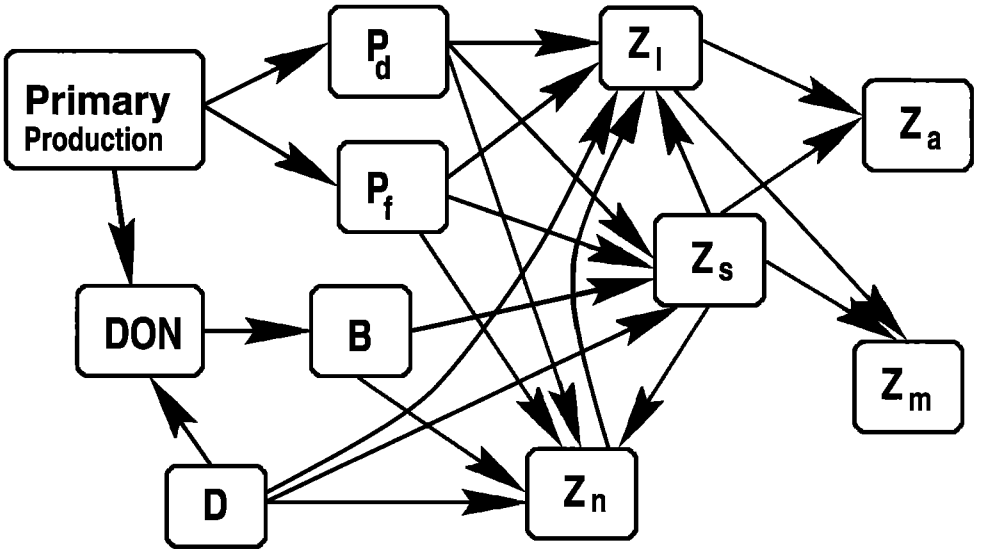


**Figure 2a.** Schematic representation of the main prey-predator interactions included into the model. In the figure, $D$ and DON denote the particulate and dissolved organic matter, and $P_d$, $P_f$, $B$, $Z_s$, $Z_l$, $Z_n$, $Z_a$, and $Z_m$ refer to diatoms, flagellates, bacteria, microzooplankton, omnivorous mesozooplankton, *Noctiluca*, *Aurelia*, and *Mnemiopsis*, respectively.

the upper layer water column of the Black Sea is represented by the structure shown in Figures 2a and 2b. Figure 2a shows the main prey-predator interactions included in the model. Figure 2b presents a schematic of other interactions taking place between the model compartments. The first trophic level of the food web consists of primary producers represented in two main functional groups: diatoms $P_d$ and nondiatom autotrophs $P_f$ (mainly flagellates). The merits of having two different phytoplankton groups for the Black Sea ecosystem were discussed previously by *Oguz et al.* [1999] (see *Andersen et al.* [1990], *Aksnes and Lie* [1990], and *Varela et al.* [1995] for similar applications). The second trophic level has microzooplankton $Z_s$ (<0.2 mm) and mesozooplankton $Z_l$ (0.2-3 mm) communities. The microzooplankton group represents heterotrophic flagellates and ciliates. It is more efficient at consuming flagellates and bacteria and links the microbial loop to the upper trophic levels. The mesozooplankton community includes both omnivores and carnivores. The om-

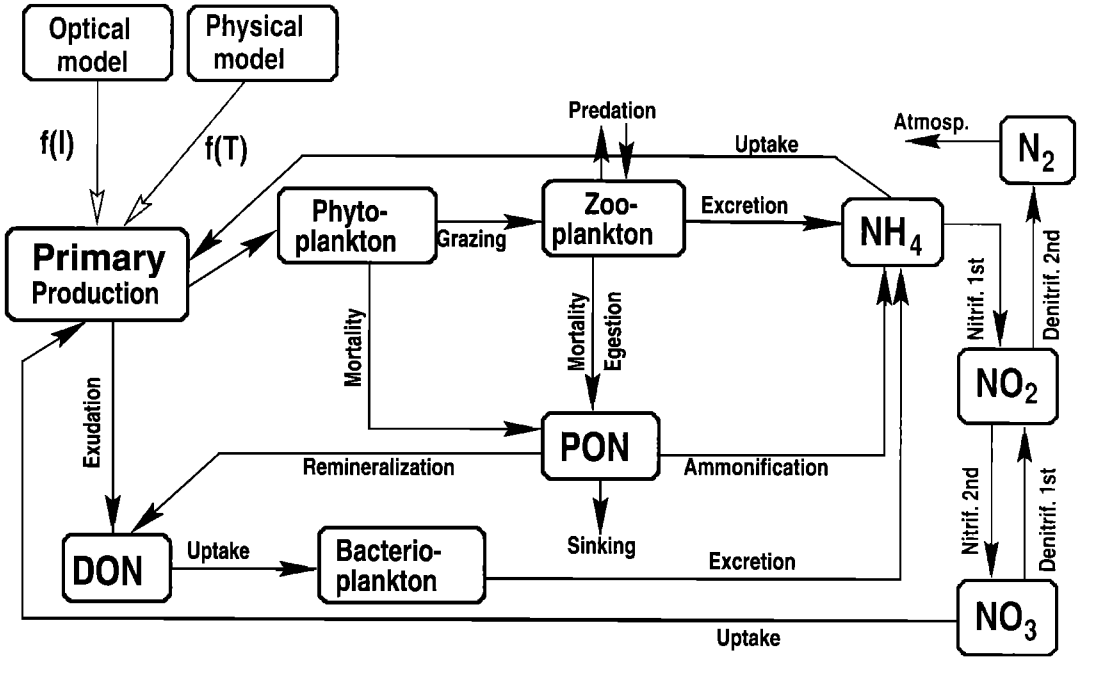


**Figure 2b.** Schematic representation of major processes and interactions between the model compartments. Details of the predator-prey relationships are shown in Figure 2a.

nivorous group is formed by young and adult individuals of copepods (e.g., *Paracalanus*, *Psedocalanus*, *Calanus*, *Acartia*, and *Oithona*), cladocerans, and appendicularians. The carnivorous group covers essentially the jellyfish *Aurelia* $Z_a$ and the ctenophore *Mnemiopsis* $Z_m$.

The model food web structure identifies the omnivorous dinoflagellate *Noctiluca* $Z_n$ as an additional independent group, which became one of the predominant species of the ecosystem during the past 2 decades [*Zaitsev and Mamaev*, 1997]. *Noctiluca* is a nonspecific consumer feeding on phytoplankton, bacteria, and microzooplankton, as well as particulate organic matter, and is consumed by mesozooplankton. The trophic structure further includes bacterioplankton $B$, labile pelagic detritus $D$, and dissolved organic nitrogen DON. Nitrogen cycling is resolved into its three inorganic forms; nitrate $NO_3$, nitrite $NO_2$, and ammonium $NH_4$. Nitrogen is considered as the only limiting nutrient for phytoplankton growth. Silicate seems not to be the limiting nutrient for diatom growth within the interior Black Sea [*Tugrul et al.*, 1992] and therefore is not taken into account in the model.

As the model is an extension of the previous model given by *Oguz et al.* [1998a], we retain the dissolved oxygen $O_2$ as an additional state variable here. The oxygen is coupled with the water column biochemistry through oxygen-dependent formulations of nitrification, denitrification, and remineralization. However, the model assumes no direct effect of oxygen on the zooplankton community. Oxygen is not a crucially important aspect of the present study.

### 2.2. Governing Equations

As by *Oguz et al.* [1996, 1998a, 1999, 2000], the local temporal variations of all variables are expressed by equations of the general form

$$\frac{\partial F}{\partial t} + \frac{\partial (w_b F)}{\partial z} = \frac{\partial}{\partial z}\left[(K_b + \nu_b)\frac{\partial F}{\partial z}\right] + \Re(F), \quad (1)$$

where $t$ is time, $z$ is the vertical coordinate, $\partial$ denotes partial differentiation, $K_b$ is the vertical turbulent diffusion coefficient, and $\nu_b$ is its background value. Here $w_b$ represents the sinking velocity for diatoms and detrital material and is set to zero for the other compartments. The interaction term, $\Re(F)$, is expressed as a balance of sources and sinks each of the biological variables.

The physical model, which is coupled with the biological model through temperature and vertical diffusivity, is based on the one-dimensional version of the Princeton Ocean Model implemented for the Black Sea. The value of $K_b(z,t)$ is computed from the physical model of mixed layer dynamics using the Mellor-Yamada level 2.5 turbulence closure parameterization. Given the daily climatological wind stress and surface buoyancy forcing throughout the year, the model computes first the physical properties of the mixed layer structure (currents, temperature, and salinity). They are then used to determine the intensity of the vertical mixing and the vertical profile of the eddy diffusivity at each time step. Within the mixed layer the computed $K_b(z,t)$ profiles indicate almost 3 orders of magnitude change during the year depending on the intensity of turbulent mixing [cf. *Oguz et al.*, 1999, Figure 6b]. For the background value of the vertical diffusivity we take $\nu_b = 2 \times 10^{-5}$ $m^2\ s^{-1}$ within the upper 60 m, decreasing linearly to $2 \times 10^{-6}$ $m^2\ s^{-1}$ at 75 m, and then we retain this value within the rest of the water column. This choice of $\nu_b$ at subsurface levels of the model is consistent with values derived from the *Gargett* [1984] formula as well as microstructure measurements [*Gregg and Ozsoy*, 1999]. It provides a reasonably adequate representation of the vertical biochemical structure consistent with observations [*Oguz et al.*, 1998a, 2001].

The annual cycle of the upper layer temperature structure simulated by the model under climatological physical forcing was described by *Oguz et al.* [1999] and will be presented here only briefly. Surface temperatures are the coldest (about 6°C) within the mixed layer of 50-75 m during January-February. By the onset of spring warming, mixed layer temperature increases gradually up to 25°C in July-August. The mixed layer is typically <20 m in this period. It is separated from colder subsurface water, which is the remnant of convectively formed cold water in the previous winter, by a very sharp seasonal thermocline during the warming cycle of the upper layer temperature structure.

Since the main focus of this paper is on predator-prey dynamics among phytoplankton and zooplankton, we first describe here the source-sink terms for the phytoplankton and zooplankton groups. Further details on formulation of other water column processes and biogeochemical cycling are given in Appendix A. Variations of the diatom and flagellate biomass are governed by

$$\Re(P_f) = (1-\chi)\sigma_f \Phi f_p(T) P_f - G_s(P_f)Z_s - G_l(P_f)Z_l - G_n(P_f)Z_n - \lambda_f {P_f}^2, \quad (2)$$

$$\Re(P_d) = (1-\chi)\sigma_d \Phi f_p(T) P_d - G_s(P_d)Z_s - G_l(P_d)Z_l - G_n(P_d)Z_n - \lambda_d {P_d}^2, \quad (3)$$

$$\Re(Z_s) = \gamma_s[G_s(P_f) + G_s(P_d) + G_s(D) + G_s(B)]Z_s - [G_l(Z_s)Z_l + G_a(Z_s)Z_a + G_m(Z_s)Z_m + G_n(Z_s)Z_n] - \mu_s Z_s - \lambda_s Z_s, \quad (4)$$

$$\Re(Z_l) = \gamma_l[G_l(P_f) + G_l(P_d) + G_l(D) + G_l(Z_s) + G_l(Z_n)]Z_l - G_a(Z_l)Z_a - G_m(Z_l)Z_m - \mu_l Z_l - \lambda_l Z_l, \quad (5)$$

$$\Re(Z_n) = \gamma_n[G_n(Z_s) + G_n(P_f) + G_n(P_d) + G_n(D)]Z_n - G_n(Z_n)Z_l - \mu_n Z_n - \lambda_n Z_n, \quad (6)$$

$$\Re(Z_a) = \gamma_a[G_a(Z_s) + G_a(Z_l)]Z_a - \mu_a Z_a - \lambda_a Z_a, \quad (7)$$

**Table 2.** Parameters of the Biological Model Used in the Simulations

| Parameter | Definition | Value |
|---|---|---|
| $a$ | photosynthesis efficiency parameter | 0.01 $m^2$ $W^{-1}$ |
| $k_w$ | light extinction coefficient | 0.08 $m^{-1}$ |
| $k_c$ | phytoplankton self-shading coefficient | 0.07 $m^2$ (mmol N)$^{-1}$ |
| $R_n$ | half-saturation constant in nitrate uptake | 0.5 mmol N $m^{-3}$ |
| $R_a$ | half-saturation constant in ammonium uptake | 0.2 mmol N $m^{-3}$ |
| $R_d$ | half-saturation constant for detrital sinking | 0.25 mmol N $m^{-3}$ |
| $R_p$ | half-saturation constant for diatom sinking | 0.5 mmol N $m^{-3}$ |
| $\psi$ | ammonium inhibition parameter of nitrate uptake | 3 (mmol N $m^{-3}$)$^{-1}$ |
| $\epsilon$ | detritus decomposition rates | 0.1 $d^{-1}$ |
| $\chi$ | exudation rate | 0.05 |
| $\kappa$ | fraction of detritus remineralization directly converted to ammonium | 0.7 |
| $w_d^*$ | maximum detrital sinking rate | 6.0 m $d^{-1}$ |
| $w_p^*$ | maximum diatom sinking rate | 1.0 m $d^{-1}$ |
| $k_1$ | maximum ammonium oxidation rate | 0.1 $d^{-1}$ |
| $k_2$ | maximum nitrite oxidation rate | 0.25 $d^{-1}$ |
| $k_3$ | maximum nitrate reduction rate | 0.015 $d^{-1}$ |
| $k_4$ | maximum nitrite reduction rate | 0.01 $d^{-1}$ |

$$\Re(Z_m) = \gamma_m[G_m(Z_s) + G_m(Z_l)]Z_m - \mu_m Z_m - \lambda_m Z_m. \quad (8)$$

According to (2) and (3) a balance between net primary production (the first terms on the right-hand sides) and losses due to zooplankton grazing (the middle terms) and physiological mortality (the last terms) controls temporal variations in the phytoplankton biomass. A fraction of growth, represented by the parameter $\chi$, is exuded as dissolved organic nitrogen. The maximum growth rate is limited by the temperature limitation function $f_p(T)$ and the factor $\Phi$ defined by the minimum of the light and nitrogen limitation terms, $\alpha(I)$ and $\beta_t(NO_3, NH_4)$, respectively. The latter is given as the sum of nitrate limitation function $\beta_n(NO_3)$ and the ammonium limitation function $\beta_a(NH_4)$. Their functional forms and other related details were presented by *Oguz et al.* [1996, 1999, 2000]. Temperature control of the maximum growth rate is expressed by the function

$$f_p(T) = Q_{10p}^{(T-20)/10} \quad (9)$$

where $T$ denotes the temperature. Definition of parameters and their values used in the model simulations are given in Table 2 and Table 3.

Changes in the zooplankton biomass are controlled by ingestion, predation, mortality, and excretion. Ingestion is represented in (4)-(8) by the terms inside the square brackets multiplied with $\gamma_i$s defining the assimilation efficiencies for grazing. The subsequent four terms inside the square brackets in (4) represent removal via predation by other groups. Similar predation terms also follow the ingestion terms in (5) and (6). The last two terms of (4)-(8) define excretion and physiological mortalities, respectively. We note that the phytoplankton mortalities are expressed in the quadratic form for stability reasons.

The grazing terms $G_i(Z_j)$s, given in (2)-(8) for all the zooplankton groups except the gelatinous carnivores, are expressed by the Michaelis-Menten relation

$$G_i(F_j) = r_i f_i(T) \frac{a_j F_j}{R_i + \sum_n a_n F_n} \quad (10)$$

where $r_i$ represents the maximum grazing rate of the $i$th consumer, and $a_j$ is food capture efficiency (i.e., food preference) of the $i$th consumer for the $j$th food item with biomass $F_j$. The efficiency parameters vary between 0 and 1, with higher values signifying greater preference. Accordingly, the maximum grazing rate $r_i$ is controlled by the temperature, half-saturation constant

**Table 3.** Parameters of the Biological Model Used in the Simulations

| Parameter | Definition | $P_d$ | $P_f$ | $Z_s$ | $Z_l$ | $Z_n$ | $Z_a$ | $Z_m$ | $B$ |
|---|---|---|---|---|---|---|---|---|---|
| $Q_{10}$ | $Q_{10}$ parameter in $f(T)$ | 1.2 | 1.2 | 2.0 | 2.0 | 2.0 | 2.2 | 2.2 | 2.5 |
| $\sigma_i$, $r_g$ | maximum growth and ingestion rates | 2.9 | 2.0 | 2.0 | 1.3 | 1.0 | fitted | fitted | 3.2 |
| $\lambda_i$ | mortality rates | 0.06 | 0.08 | 0.04 | 0.04 | 0.08 | 0.002 | 0.002 | - |
| $\mu_i$ | excretion rates | - | - | 0.07 | 0.07 | 0.08 | 0.03 | 0.03 | 0.08 |
| $\gamma_i$ | assimilation efficiencies | - | - | 0.75 | 0.75 | 0.80 | 0.80 | 0.80 | - |
| $R_i$ | half-saturation constant | - | - | 0.5 | 0.4 | 0.5 | 0.7 | 0.50 | 0.75 |

**Table 4.** Food Capture Efficiency Coefficients

| | Predator | | | | | |
|---|---|---|---|---|---|---|
| Prey | $Z_s$ | $Z_l$ | $Z_n$ | $Z_a$ | $Z_m$ | $B$ |
| $P_f$ | 0.7 | 0.2 | 0.9 | - | - | - |
| $P_d$ | 0.2 | 1.0 | 0.35 | - | - | - |
| $Z_s$ | | 0.7 | 0.2 | 0.2 | 0.2 | - |
| $Z_l$ | - | - | - | 1.0 | 1.0 | - |
| $Z_n$ | - | 0.2 | - | - | - | - |
| $B$ | 1.0 | 0.1 | - | - | - | - |
| $D$ | 1.0 | 0.7 | 0.2 | - | - | 0.2 |
| DON | - | - | - | - | - | 1.0 |

$R_i$, and food capture efficiencies. The values of food capture efficiency parameters for each prey-predator couple are given in Table 4. The temperature limitation function $f_i(T)$ is expressed by (9).

As stated in section 2.1, the focus of this paper is not to explore the life history characteristics of the gelatinous zooplankton by implementing a population dynamics model, like the one provided by *Volovik et al.* [1995] for the Azov Sea. We intend here to study how the annual distributions of phytoplankton and mesozooplankton distributions are altered by top-down control imposed by these gelatinous carnivores. The simplest approach is to formulate their grazing pressures diagnostically using their observed annual biomass distributions and a functional relationship, which designates the predation impact of this biomass on the phytoplankton and zooplankton [e.g., *Kremer and Nixon*, 1978]. In this case the model does not require explicitly (7) and (8) for simulating the temporal changes of their biomass as a result of source/sink terms. In the case of our depth dependent vertically resolved model, however, this approach cannot be used since the biomass data do not include depth distributions and are only given in the form of vertically integrated values (see Figure 1 and Table 1). Therefore (7) and (8) are used to predict their biomass prognostically within the water column.

The Michaelis-Menten-type representation of grazing is not appropriate for *Aurelia* and *Mnemiopsis*. Experimental data [e.g., *Reeve et al.*, 1992; *Kremer*, 1977; *Finenko et al.*, 1995] showed that they do not satiate at reasonable concentrations of prey and that they continue to destroy prey even when they are not digested. *Kremer* [1976a] represented ingestion by ctenophores in terms of clearance rate (depending on size of ctenophores and temperatures) and linearly varying prey biomass. In the present model we thus express grazing of the gelatinous carnivores by [see *Eeckhout and Lancelot*, 1997]

$$G_i(F_j) = r_i(t) a_j F_j, \tag{11}$$

where the subscript $i$ denotes either $a$ for *Aurelia* or $m$ for *Mnemiopsis* and $F_j$ represents the biomass of the $j$th prey. The time dependent forms of $r_i(t)$ parameterize clearance rates, which were not modeled explicitly and are prescribed externally in such a way that the annual biomass distributions of ctenophores are predicted consistent with available data. This approach is similar to the one given by *Fasham et al.* [1999], where the bacterial and primary production were prescribed as given forcing inputs in order to quantify various pathways of carbon flow within the euphotic zone. We note that *Fasham et al.* [1999] used the hybrid approach to close the ecosystem at the lowest level, whereas in our case it is used for closure at the highest trophic level.

### 2.3. Boundary and Initial Conditions, and Numerical Procedure

The bottom boundary of the model is taken at a depth of 150 m. This roughly corresponds to the base of the permanent pycnocline and is chosen to be reasonably removed from the domain of interest in this model study. The physical model is forced by monthly climatological wind stress and surface thermal fluxes [see *Oguz et al.*, 1996, Table 2] whereas no-stress, no-heat, and no-salt flux conditions are specified at the bottom. For the biochemical model the turbulent fluxes are set to zero at the surface and bottom boundaries for all the state variables. In the diatom and detritus equations, no-diffusive flux conditions at the bottom boundary are modified to include the absence of sinking particulate matter and diatom fluxes. The condition of no sinking detrital flux across the bottom boundary implies its complete remineralization within the upper 150 m of the water column. The assumption of complete remineralization is supported by sediment trap observations, which indicate about 10% loss to the lower layer of the Black Sea. Further justification and details on the bottom boundary conditions are given by *Oguz et al.* [1996, 1999, 2000].

The physical model is initialized by stably stratified upper ocean temperature and salinity profiles representative of autumn conditions for the interior part of the sea. The biochemical model does not possess any prescribed a priori vertical structure. It is initialized by assigning a vertically uniform nitrogen (3.5 $\mu$M nitrate and 0.5 $\mu$M ammonium) source in the water column. Small constant values are prescribed for the other state variables. Our simulations are therefore independent of initial conditions. As there is no nitrate input into the water column across the boundaries, the model utilizes the initial nitrogen stock to generate living and nonliving components of the biological system by the internal dynamical processes incorporated into the model. The model has a small loss of nitrogen flux of $k_4 f_d(O_2)NO_2$ at each time step because of denitrification taking place within the oxygen deficient zone of the model.

The details of the numerical solution procedure were described by *Oguz et al.* [1996]. A total of 50 vertical levels is used to resolve the 150 m thick water column. A time step of 5 min is used in the numerical integration of the system of equations. First, the physical model

is integrated for 5 years to achieve a stable annual cycle of the upper layer physical structure. Using these results, the biochemical model is first integrated for 2 years to accomplish its transient adjustment from the initial conditions. The integration is then carried out for 2 more years by including an equivalent nitrogen flux at the level of the nitrate maximum to compensate for the loss due to denitrification, $k_4 f_d(O_2)NO_2$, at each time step. Within the limitations of the one-dimensional model, specifying the compensatory nitrogen flux at the level of the nitrate maximum appears to be a reasonable choice. The results presented here are based on the fourth year of integration. Time integration starts from October, and the perpetual year in the model covers the period from October 1 to September 30. The solutions are, however, presented by starting from January 1.

## 3. Simulation of the *Aurelia*-Dominated Ecosystem and Its Validation Against 1978 Gelendzhik Data

In this section, using a specific data set, we explore conditions of the perturbed ecosystem during the late 1970s due to population increase of gelatinous organisms (*Aurelia* and *Pleurobrachia*) and the opportunistic species *Noctiluca*. The data set also provides a unique opportunity to demonstrate how well the model simulates the general pattern of the observed sequence of events, given a paucity of seasonally resolving data sets for the region. The data comprise all together 20 sets of in situ measurements of bacterioplankton, mesozooplankton, microzooplankton, and phytoplankton taken at 2-4 week intervals during 1978 at an offshore station situated approximately at 44.5° N, 38° E, off Gelendzhik along the Caucasian coast [*Shushkina et al.*, 1983]. The data set tends to represent conditions of the interior basin ecosystem, modified to a certain extent by the regional component of the basinwide Rim Current system. To our knowledge, this is a unique time series data set involving simultaneous measurements of several variables over a single one year period. The validation exercises in our earlier models [*Oguz et al.*, 1996, 1998a, 1999] were based on composite annual time series data of plankton biomass, chlorophyll *a* and primary production constructed by combining measurements made in different months of different years [*Vedernikov and Demidov*, 1993, 1997; *Shuskina et al.*, 1998]. These composite data sets will also be used here to complement observations not included in the 1978 Gelendzhik data set.

There are several simplifications and idealizations used in the model that may affect the fidelity of the simulations. First, the physical model is forced by climatological data rather than those specified particularly for the year 1978. Then, the biological model is initialized by a set of idealized conditions not representing the observed structure at the beginning of the simulation period. Moreover, the food web structure shown in Figure 2a without the *Mnemiopsis* compartment may be simpler than necessary to provide a realistic representation of the Gelendzhik 1978 ecosystem. On the other hand, we would like to emphasize that reproduction of all the details of the data is not our major intention here. The main motivation of this calibration/validation exercise is to show how this relatively simple process-oriented model is appropriate for studying ecosystem changes of the past several decades in the Black Sea.

### 3.1. Setting Biological Parameters

Given the variability in the observations and uncertainties in the choice of some input parameters of the model, it is unrealistic to expect a unique set of parameters providing a good fit of the model to the observations. The observations and experiments performed on different cruises by the Shirshov Institute of Oceanology provide a basis for setting values for the input parameters (Tables 2-4). We also benefited from parameter settings used by other Black Sea ecosystem modeling studies [e.g., *Belyaev and Konduforova*, 1992; *Lebedeva and Shushkina*, 1994; *Eeckhout and Lancelot*, 1997]. The choices for most of the parameters concerning the phytoplankton, microzooplankton, and mesozooplankton compartments were discussed by *Oguz et al.* [1996, 1998a, 1999]. The coefficients of food preferences (Table 4) are known only approximately from available observations indicating major prey consumption for *Aurelia* on mesozooplankton [*Sullivan et al.*, 1994], to a lesser extent on microzooplankton [*Stoecker et al.*, 1987], and for *Mnemiopsis* primarily on mesozooplankton [*Purcell et al.*, 1994b]. Since sensitivity experiments suggested their strong influence on the model results, they were treated as free parameters in the sense that they were optimized to yield an acceptable fit to the Gelendzhik data. They were then kept unchanged in the other experiments.

### 3.2. Observed Variations of Plankton Stocks

The observed distributions of total phytoplankton and mesozooplankton biomass during January-December 1978 (expressed in gC $m^{-2}$) are shown in Figure 3a. The data may suffer from inadequate sampling resolution at some periods of the year but provide a plausible annual structure. The March to early April period corresponded to the formation of major phytoplankton and subsequent mesozooplankton blooms. As noted previously by *Oguz et al.* [1996, 1998a, 1999], these blooms were the most robust signatures of the annual plankton structure of the Black Sea ecosystem, seen in every data set [e.g., *Sorokin*, 1983; *Vedernikov and Demidov*, 1997]. The late spring to early summer season was characterized by relatively lower biomass values of both phytoplankton and mesozooplankton. This period was followed by successive peaks of mesozooplankton and phytoplankton at the end of the summer season. Bacteria and microzooplankton biomass, which were also

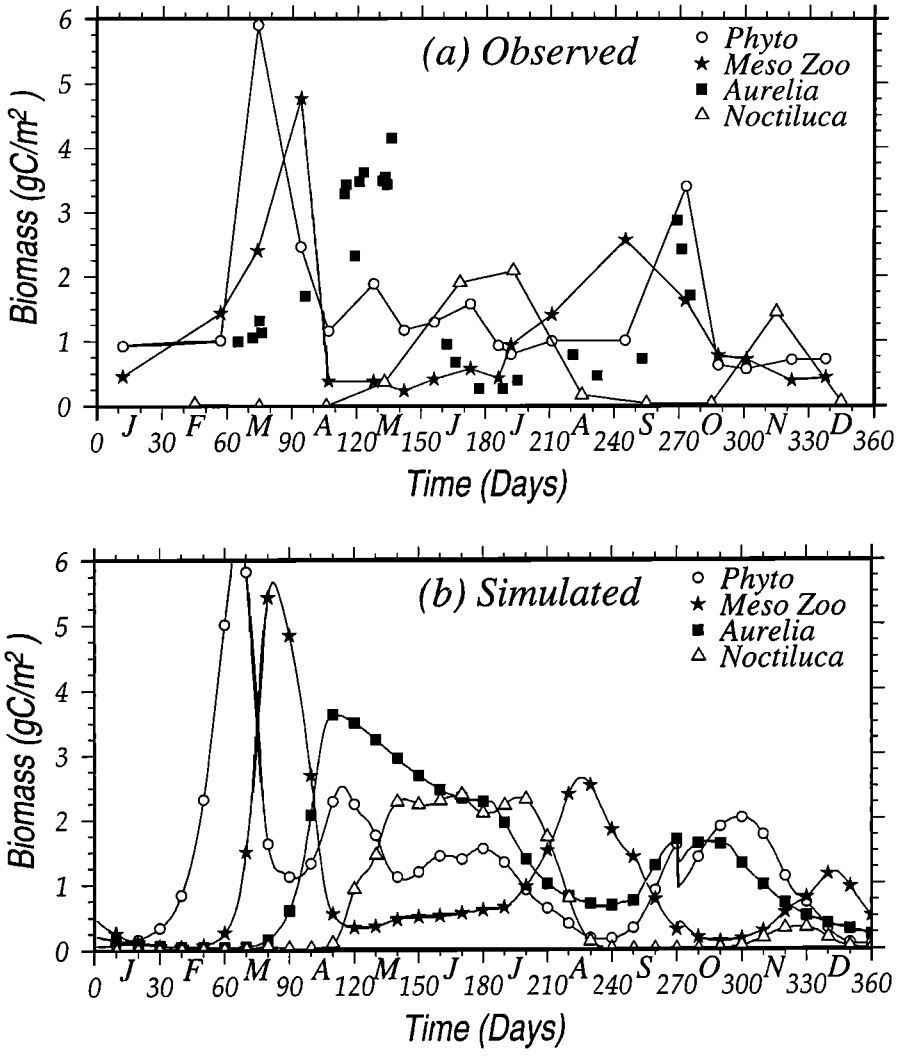


**Figure 3.** (a) Observed and (b) Simulated annual distributions of total phytoplankton, mesozooplankton, *Noctiluca*, and *Aurelia* biomass. The data for phytoplankton and mesozooplankton biomass are taken from the measurements carried out at 2-4 week intervals during January-December 1978 at an offshore station off Gelendzhik along the Caucasian coast. The *Noctiluca* and *Aurelia* biomass data are taken from measurements on the Romanian shelf and the interior basin, respectively, during the late 1970s and early 1980s. (*Noctiluca* and *Aurelia* distributions are reproduced from their originals, using the data provided by *Eeckhout and Lancelot* [1997] and *Shushkina et al.* [1998], respectively).

measured but not shown here, stayed at much lower levels than the other groups and did not show any appreciable variation throughout the year.

The presence of spring and autumn phytoplankton peaks in the 1978 Gelendzhik data is also supported by other independent data sets from the 1980s. Figure 4 shows the annual surface chlorophyll distributions for the western and eastern basins derived from the 1979-1985 composite Coastal Zone Color Scanner (CZCS) imagery and from the in situ data within the interior parts of the basin during approximately the same period.

Unfortunately, the Gelendzhik 1978 data set does not provide an annual time series for *Noctiluca* or *Aurelia*. However, some other complementary data sets are available and might be used to provide partial support for the model's performance. Figure 3a also shows the annual biomass distribution of *Noctiluca* within the offshore waters of the Romanian shelf for the early 1980s' ecosystem representing conditions after major ecosystem changes took place in the Black Sea. The *Noctiluca* possesses two particular periods of increased biomass in midsummer and midautumn, with the former being the major one. *Aurelia* biomass, on the other hand, is characterized by late spring to early summer (around May) and autumn (around October) peaks and a minimum in July-August (Figure 3a; see also Figure 1 and Table 1).

### 3.3. Simulation of Gelendzhik 1978 Ecosystem

Despite the uncertainties in the initial conditions and meteorological forcing, neglecting a possible contribution of advective influence by the Rim Current and a

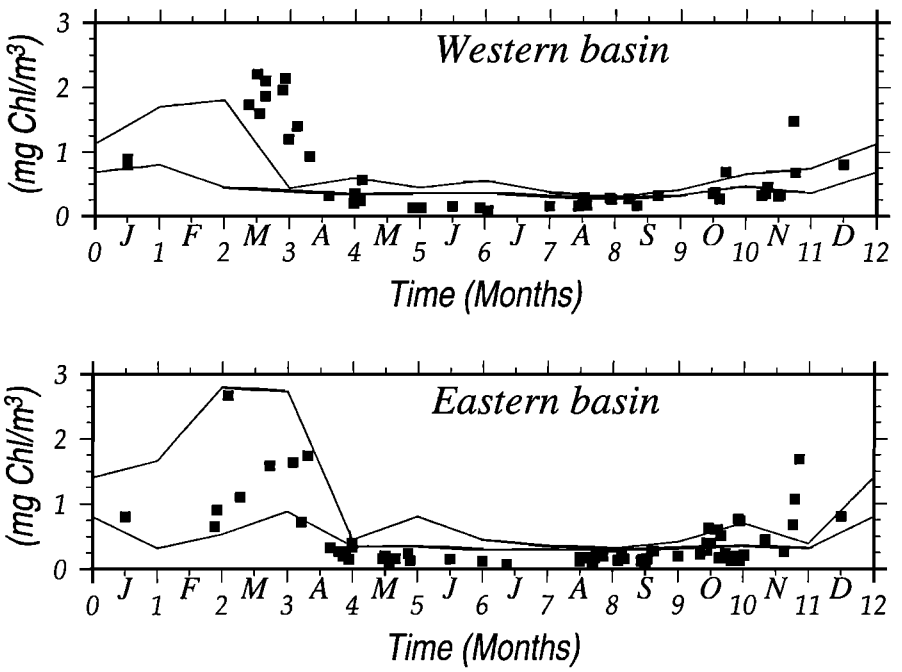


**Figure 4.** The annual distributions of surface chlorophyll (mg $m^{-3}$) in the western and eastern basins of the Black Sea. Solid lines represent the range of variations confined between the 25th and 75th percentiles of values derived from the monthly composite CZCS imagery for the 1979-1985 period. The solid squares are composite values from the in situ field measurements within the central Black Sea during the 1980s. This figure is reproduced from its original, using the data provided by *Nezlin et al.* [1999]

lack of complete knowledge of major trophic interactions between different levels of the zooplankton community, the observed (Figure 3a) and simulated (Figure 3b) annual cycles of the plankton biomass reveal as much similarity as one could reasonably expect from such a simplified model. The results are computed in units of mmol N and then converted to carbon units using the carbon to nitrogen ratio of 8.0 adopted by *Oguz et al.* [1996]. This ratio is set to 4.0 for *Aurelia* and *Mnemiopsis*, as being typical for gelatinous and crustacean zooplankton [*Kremer*, 1976a; *Purcell and Kremer*, 1983; *Larson*, 1986]. The model simulation reproduces the observed March-April and September-October phytoplankton and mesozooplankton biomass peaks fairly well in terms of both their timing and their intensity. The bacterioplankton and microzooplankton biomass distributions are also simulated reasonably well during the year (not shown).

The late winter (February) increase in phytoplankton biomass is associated with a classical new production-based diatom bloom. It is the strongest bloom event of the year because of the high rate of nitrate entrainment into the mixed layer as a result of intense convective mixing prior to the bloom event. The nitrate distribution (Figure 5a) reveals accumulation up to 2.5 mmol $m^{-3}$ within the mixed layer during January and the first half of February. As the zooplankton biomass controlling the phytoplankton community nearly vanishes (see Figure 3b) and the water column acquires a net growth rate (Figure 6) toward the end of January, the phytoplankton biomass begins to increase gradually. The balance between the time rate of change of diatom biomass and the net production rate then leads to exponential growth toward the end of February. The surface intensification of the bloom at the beginning of March (Figure 5c) is related to the larger contribution of the light limitation function to net growth rate near the surface. The net growth rate decreases from the maximum value of ~0.4 $d^{-1}$ at the surface to 0.1 $d^{-1}$ at 20 m depth.

As the bloom terminates toward the end of March, the remineralization-ammonification-nitrification cycle introduces considerable regenerated nutrient in the form of ammonium and nitrate both above and below the seasonal thermocline (Figures 5a and 5b). Although the base of the mixed layer is best identified by the temperature structure [see *Oguz et al.*, 1999, Figure 6a], we infer it here by the sharp nitrate variations near the surface. Nitrate and ammonium trapped within the upper 15 m during late March and early April are utilized during the surface-intensified bloom event within the second week of April. Once the mixed layer nutrient stocks are depleted, this event continues to take place at subsurface levels between the seasonal thermocline and the base of the euphotic zone during the rest of the summer (Figure 5c).

The modeled distribution of *Aurelia* in the Black Sea is characterized by two major periods of increased

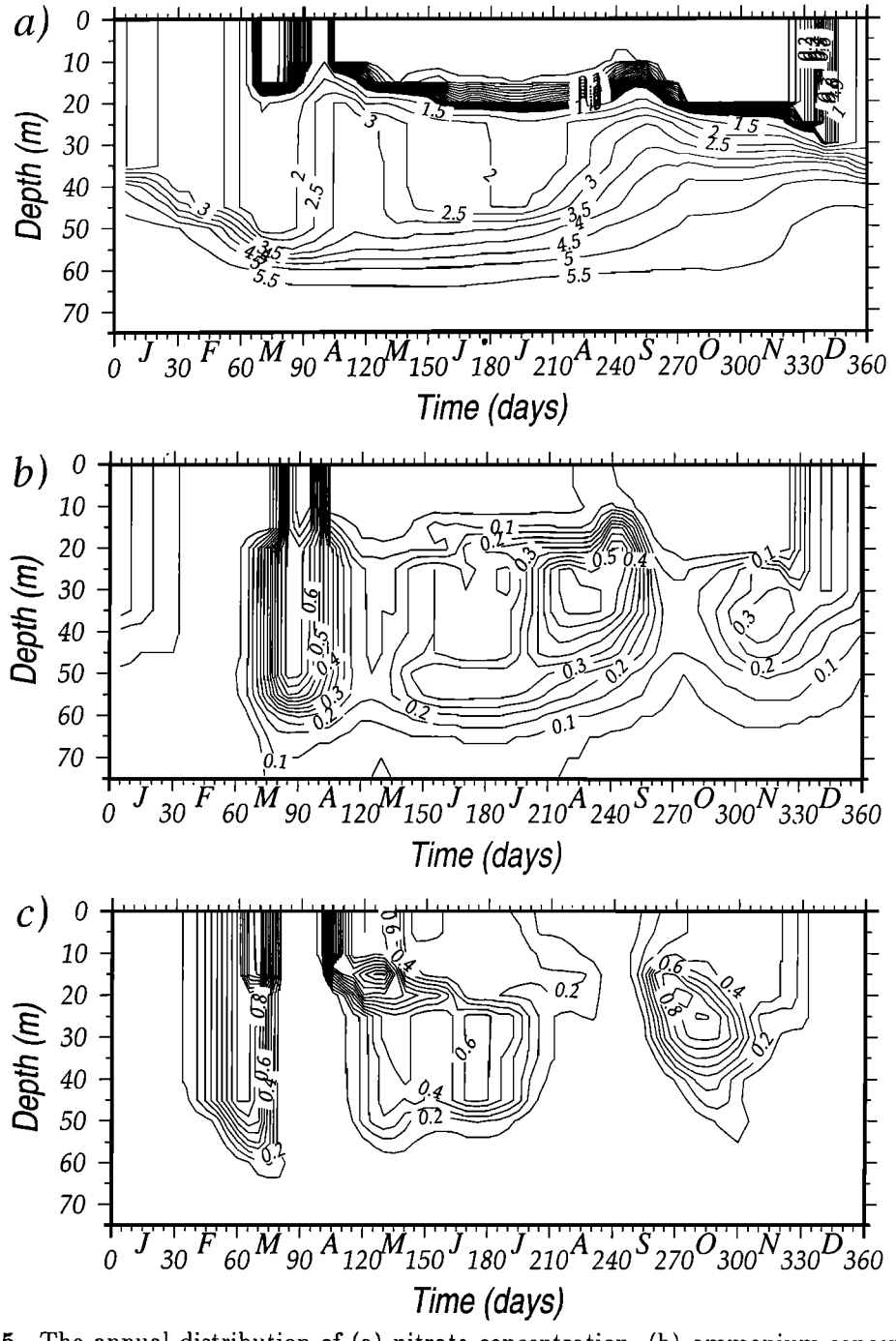


**Figure 5.** The annual distribution of (a) nitrate concentration, (b) ammonium concentration, and (c) total phytoplankton biomass within the upper layer water column computed for model ecosystem conditions of the late 1970s and early 1980s prior to mass development of *Mnemiopsis*. The units are given in mmol N $m^{-3}$. The contours are drawn at intervals of 0.1 up to 1.0 mmol N $m^{-3}$ and afterwards 0.5 mmol N $m^{-3}$ for nitrate, at intervals of 0.05 mmol N $m^{-3}$ for ammonium, and at intervals of 0.1 mmol N $m^{-3}$ for total phytoplankton biomass.

biomass (Figure 3b), as suggested by the data shown in Figure 3a. Each lasts about 2 months during the late spring and autumn periods. A steady increase in biomass occurs from late April until the beginning of July. It reaches a maximum value of ~4.5 gC $m^{-2}$ as *Aurelia* deplete the entire mesozooplankton stock available to support their growth. The second increase in the population takes place at the beginning of October following a second peak of omnivorous mesozooplankton stock in the system. *Aurelia* biomass declines to a minimum level of ~1.5 gC $m^{-2}$ during July-August corresponding to the time of the summer mesozooplankton

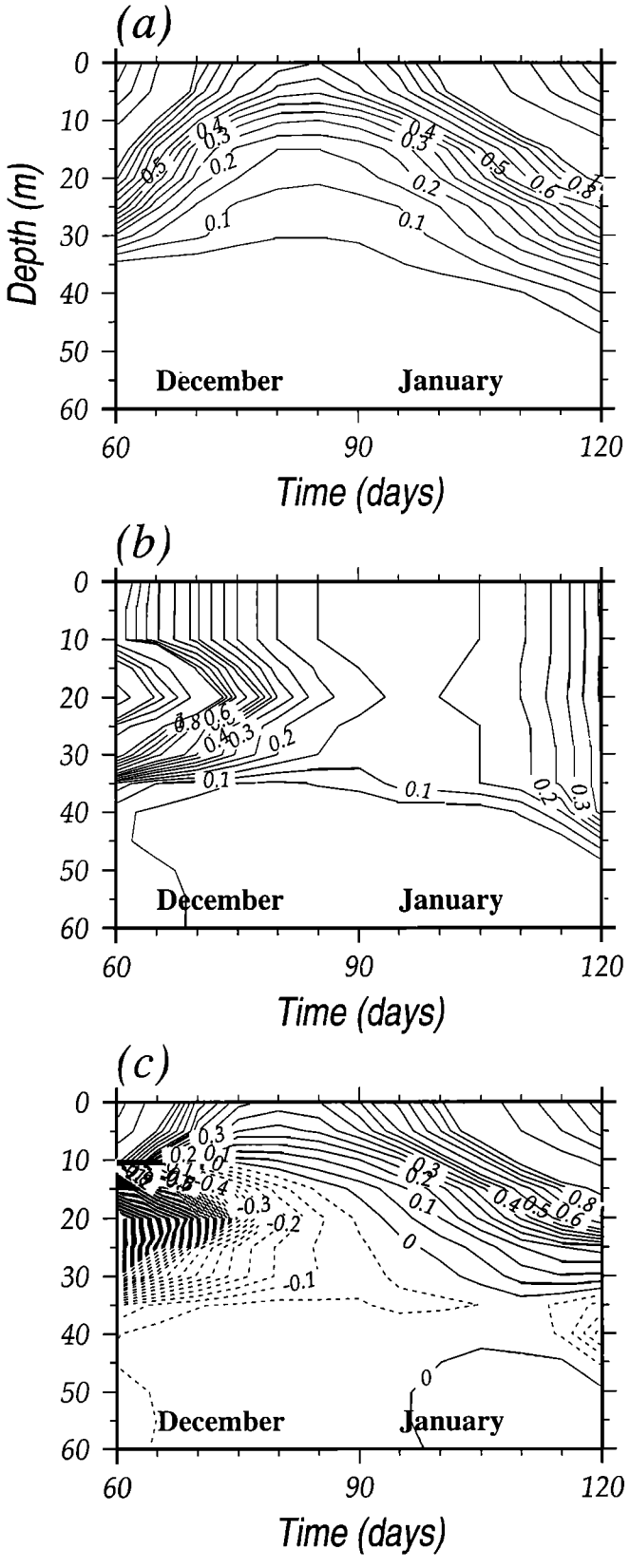


**Figure 6.** The distributions of (a) primary production, (b) total loss, and (c) primary production minus total loss terms in the diatom equation during December and January of the perpetual model year. The dashed lines in Figure 6c indicate negative values. The units are given in mmol N $m^{-3}$ $d^{-1}$. The contours are drawn at intervals of 0.05 mmol N $m^{-3}$ $d^{-1}$.

peak. The population also decays during the winter months until a new cycle of growth and reproduction begins in April. The model also reproduces increased *Noctiluca* biomass of about ~2.0 gC $m^{-2}$ during June-July. The timing of the second peak in the model is also consistent with the data, but its intensity is somewhat lower. These peaks follow the two phytoplankton blooms.

Figure 3b indicates that the peaks of phytoplankton, *Noctiluca*, *Aurelia*, and omnivorous zooplankton biomass march sequentially during the year as a result of their prey-predator interactions. After the early spring diatom bloom, the omnivorous mesozooplankton biomass starts increasing as they assimilate diatoms. Their biomass tends to decline in April, which coincides with the beginning of the period of *Aurelia* growth. At the same time, as the grazing pressure from mesozooplankton is relaxed gradually, the phytoplankton community attains two successive peaks during mid-May and June, respectively. The phytoplankton biomass then exhibits a decreasing trend during July, as they are consumed by *Noctiluca*. July therefore coincides with the annual production maximum for *Noctiluca*. The summer omnivorous mesozooplankton growth occurs right after the decline of the *Aurelia* population, as well as the decline of the phytoplankton bloom toward the end of June. Mesozooplankton biomass decreases in September during the second period of *Aurelia* growth. This period also coincides with an increase in phytoplankton stocks.

The annual biomass cycles of phytoplankton and mesozooplankton simulated above for the Gelendzhik 1978 ecosystem arise because of the specific form of grazing pressure exerted by the *Aurelia* community. In other words these annual patterns depend crucially on the particular structure of *Aurelia* biomass variations within the year. We found that it was necessary to have the summer biomass decrease of *Aurelia* between its spring and autumn peaks (Figure 3a). Otherwise, it was not possible to simulate plankton distributions consistent with the observations. For example, Figure 7 shows the results from a simulation in which we use a slightly different choice for the *Aurelia* grazing rate specification $r_a(t)$ in (11). Instead of its minimum during July-August, it sets the *Aurelia* biomass to have a more gradual decrease during summer. The new form of top-down grazing pressure introduced by this relatively higher summer *Aurelia* biomass gives rise to completely different phytoplankton, mesozooplankton, and *Noctiluca* biomass structures over the year (Figure 7), which is inconsistent with the observations.

## 4. Simulation of the *Mnemiopsis*-Dominated Ecosystem and Its Validation With the Available Data

We explore here characteristic features of the second stage (during 1989-1991) in the ecosystem, which was

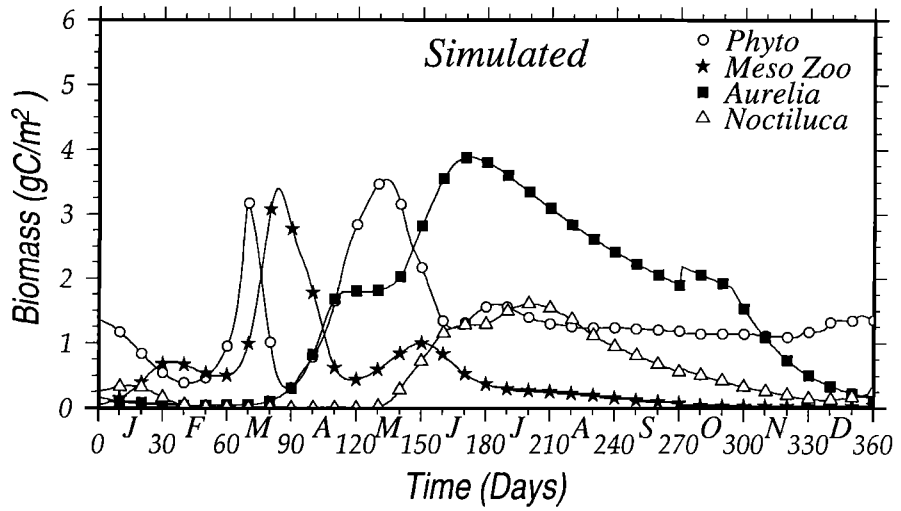


**Figure 7.** The annual cycles of phytoplankton, omnivorous mesozooplankton, *Noctiluca*, and *Aurelia* biomass (in gC $m^{-2}$) simulated using an alternative ingestion rate specification, which provides higher summer *Aurelia* biomass distribution.

dominated by mass development of *Mnemiopsis* and a dramatic reduction in *Aurelia* stocks (see Figure 1). The simulation experiment retains the entire parametric setting of the previous simulation of the 1978 Gelendzhik ecosystem but introduces an additional compartment for *Mnemiopsis* with an additional equation (8), related terms in other equations, and the relevant parameters listed in Tables 2-4.

When compared with the pre-*Mnemiopsis* case shown in Figure 3, introduction of *Mnemiopsis* into the ecosystem caused dramatic changes in all components of the food web (Figure 8). The phytoplankton distribution has now three distinct blooms within the year. The first one is the classical late winter diatom bloom as in the previous case, but it starts earlier in January and reaches its highest biomass value of ~5.5 gC $m^{-2}$ at the end of February. The second bloom period immediately follows the first one, starting at the beginning of April and lasting until mid-June, with biomass increases up to ~5.0 gC $m^{-2}$ by the end of April. The third bloom covers the late summer season from the beginning of July to the end of September. Its peak of ~3.0 gC $m^{-2}$ during early August is, however, somewhat lower than the previous blooms. The autumn season represents the least active period of the year, characterized by a gradual decrease in phytoplankton biomass until the next winter bloom in January. The vertical structure of these blooms is shown in Figure 9.

The distributions of the production and total loss terms during December and January (Figure 10) may

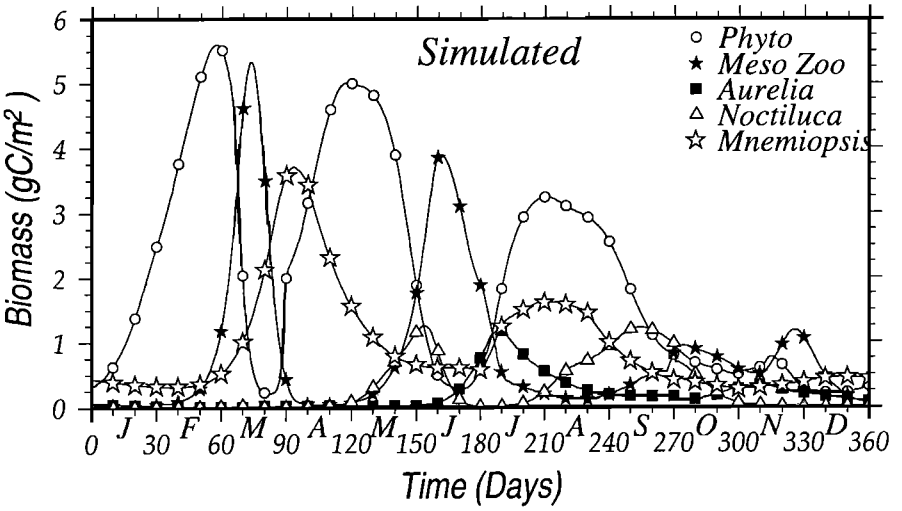


**Figure 8.** The annual cycles of phytoplankton, omnivorous mesozooplankton, *Noctiluca*, *Aurelia*, and *Mnemiopsis* biomass (in gC $m^{-2}$) simulated for the late 1980s ecosystem after mass development of *Mnemiopsis*.

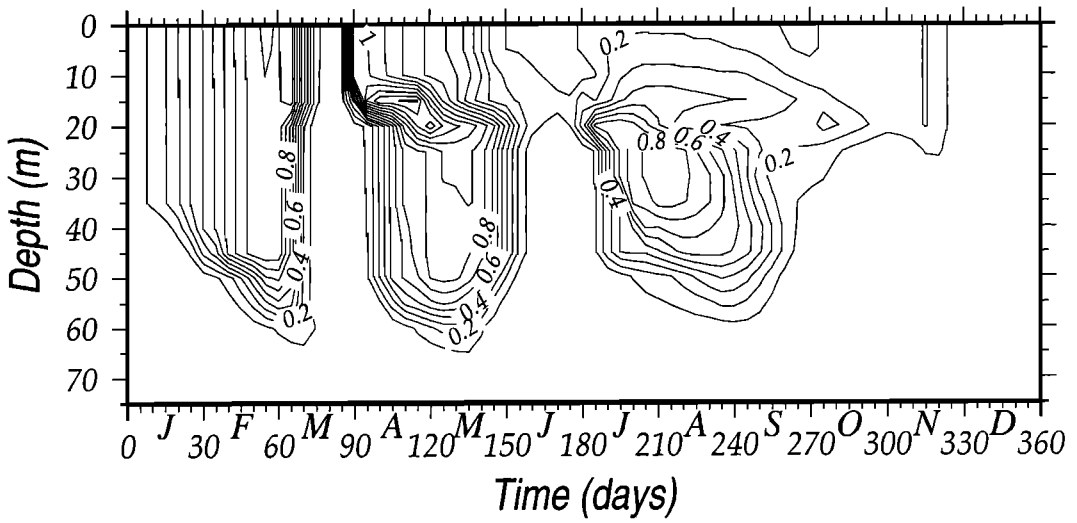


**Figure 9.** The annual distribution of total phytoplankton biomass (in mmol N $m^{-3}$) within the upper layer water column simulated for the late 1980s ecosystem after mass development of *Mnemiopsis*. The contours are drawn at intervals of 0.1 mmol N $m^{-3}$.

provide a clue for the initiation of the diatom bloom as early as January. Figure 10a indicates a gradual increase of production term at the end of December, which also represents a period of very low total loss rate in the system (Figure 10b). The net production rate (Figure 10c), which balances the time rate of change of diatom biomass, then gives rise to an increase in the biomass at the beginning of January. It is followed by exponential growth later in the month with increasing values of the net production rate.

The omnivorous mesozooplankton have two major peaks of about 5.0 gC $m^{-2}$ during mid-March and toward mid-June. They take place right after the late winter and spring phytoplankton blooms (Figure 8), respectively. The first mesozooplankton bloom lasts only 2 weeks as they are utilized immediately by *Mnemiopsis*. The second mesozooplankton peak follows the spring phytoplankton bloom event and occurs prior to the growth of *Mnemiopsis*. The mesozooplankton maintain their stocks until mid-July after which they begin to be consumed by *Mnemiopsis* as well as *Aurelia*. Some increase in the mesozooplankton stocks also takes place during the autumn season after the enhanced summer phytoplankton activity. A small peak at the end of November represents increase in mesozooplankton biomass following relaxation of gelatinous grazing pressure. Finally, *Mnemiopsis* growth in the ecosystem causes a reduction in *Noctiluca* biomass as compared with the pre-*Mnemiopsis* period. The first *Noctiluca* growth in the system occurs after mid-April and continues until the end of June, with peak biomass of 1.0 gC $m^{-2}$ toward the end of May. The period between August and October constitutes a second growth season, with peak biomass values of ~1.0 gC $m^{-2}$. The temporal distribution of bacteria do not differ much from the previous case, but the biomass peaks tend to have higher values (not shown).

The first biomass increase of *Mnemiopsis* up to ~4.0 gC $m^{-2}$ takes place toward the end of March, following the first mesozooplankton peak. Consistent with the form of the diagnostically defined growth rate, *Mnemiopsis* biomass decline gradually in April-June and is then subject to a subsequent increase toward the first half of August. We note that the period between these two *Mnemiopsis* biomass peaks corresponds to the depletion of mesozooplankton stocks and massive growth of phytoplankton in the ecosystem. *Aurelia* is no longer able to grow in this new ecosystem, except for a small peak of about 1.0 gC $m^{-2}$ during July. The near absence of *Aurelia* and the preferential consumption of mesozooplankton stocks by *Mnemiopsis* are related to the fact that *Mnemiopsis* growth and reproduction start earlier than those of *Aurelia*, immediately after the late winter phytoplankton and mesozooplankton blooms. Sensitivity experiments suggested that *Aurelia* could outcompete and/or take over *Mnemiopsis* if its growth and reproduction season started as early as those of *Mnemiopsis*. This phenomenon may explain year-to-year as well as regional variabilities observed in the spring *Aurelia* and *Mnemiopsis* stocks observed in the 1990s [e.g., *Kovalev et al.*, 1998; *Shiganova et al.*, 1998]. This issue will be a subject of future modeling studies devoted particularly to the characteristics of ecosystem changes in the 1990s.

Because the outbreak of the *Mnemiopsis* population and its competition with *Aurelia* took place in a relatively short period of time during the late 1980s and early 1990s, it is difficult to provide observational support for all components of the ecosystem throughout the year. Here we present available data to validate the late 1980s ecosystem simulation. As reported by *Kovalev and Piontkovski* [1998], the composite data formed by measurements within the interior basin during the past decade (Figure 11a) suggest an order of magnitude de-

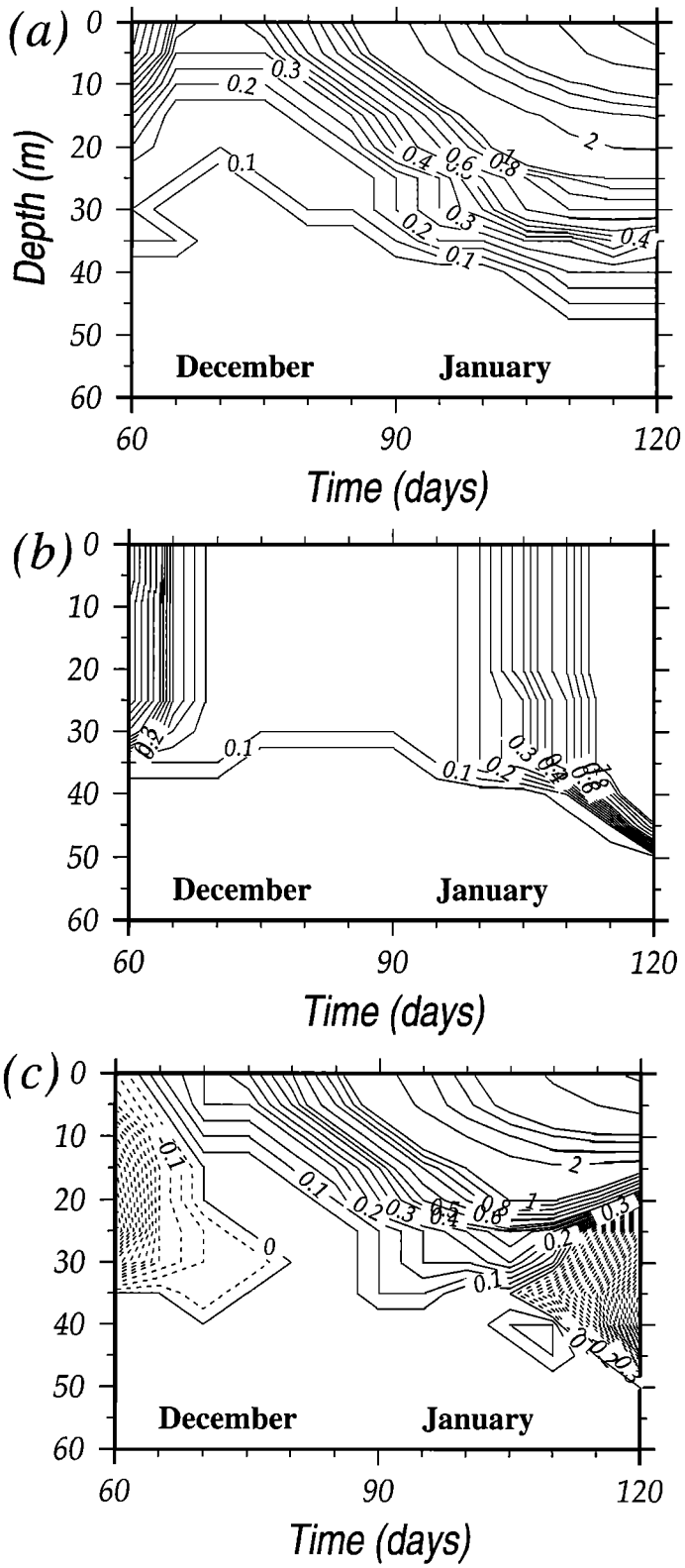


**Figure 10.** The distributions of (a) primary production, (b) total loss, and (c) primary production minus total loss terms in the diatom equation during December and January of the perpetual model year for the late 1980s ecosystem conditions after mass development of *Mnemiopsis*. The dashed lines in Figure 10c indicate negative values. The units are given in mmol N $m^{-3}$ $d^{-1}$. The contours are drawn at intervals of 0.05 mmol N $m^{-3}$ $d^{-1}$.

crease in *Noctiluca* biomass from the 1980s to the early 1990s, as also simulated by the model. More interestingly, measurements from Sevastopol Bay during 1989 and 1990 (Figure 11b) reveal similar temporal shifts of the *Noctiluca* biomass peaks to May and September, although the latter seem to be stronger than those given by the model. Furthermore, the ratio of total *Noctiluca* biomass to the total gelatinous carnivore biomass of 0.16 computed by the model is comparable with its observed value of 0.1 reported by *Kovalev and Piontkovski* [1998].

The presence of winter blooms and subsequent shifts in the timing of phytoplankton and mesozooplankton biomass are supported by direct measurements carried out within interior Black Sea waters during February-April 1991 (Figure 12). The data provided by *Shushkina et al.* [1998] indicate an increasing trend of phytoplankton biomass, reaching a value of ~6.0 gC $m^{-2}$ toward the end of February, as simulated by the model. The existing Black Sea data set does not contain similar high winter phytoplankton biomass values for the years prior to the outbreak of the *Mnemiopsis* population [*Vedernikov and Demidov*, 1993]. The data further indicate enhanced mesozooplankton stocks during March following the phytoplankton bloom, though the highest biomass values given in the data were somewhat lower than those shown in our simulations in Figure 8.

The seasonal variations of phytoplankton after the introduction of *Mnemiopsis* into the system are supported by a surface chlorophyll data set formed by combining the Turkish, Russian, Ukrainian, Bulgarian, and Romanian measurements for the period of 1990- 1995 [*Yilmaz et al.*, 1998]. The main finding from this data set was the recognition of chlorophyll peaks in winter (January-February) and in spring to early summer (May-June) (Figure 13). Even though monthly averaging should cause underestimation of peak concentrations, the data set is still able to indicate clearly the peaks simulated by the model.

## 5. Summary and Conclusions

In the Black Sea more frequent and pronounced phytoplankton blooms and sharp population increases in the gelatinous organisms (*Aurelia* and *Mnemiopsis*) and opportunistic species *Noctiluca* at the expense of mesozooplankton stocks were major consequences of severe eutrophication together with the introduction of *Mnemiopsis* and overfishing. Existing studies inferred these cause and effect relations from descriptive treatments of available data. However, because of limitations in the database (due to scarcity and insufficiency of measurements), these early analyses were inconclusive in providing a systematic explanation of the functioning of the pelagic food web during the past 2 decades. The major goal for the present work was to explore the nature of trophic interactions and then to establish quantitatively the links between components of the ecosystem at

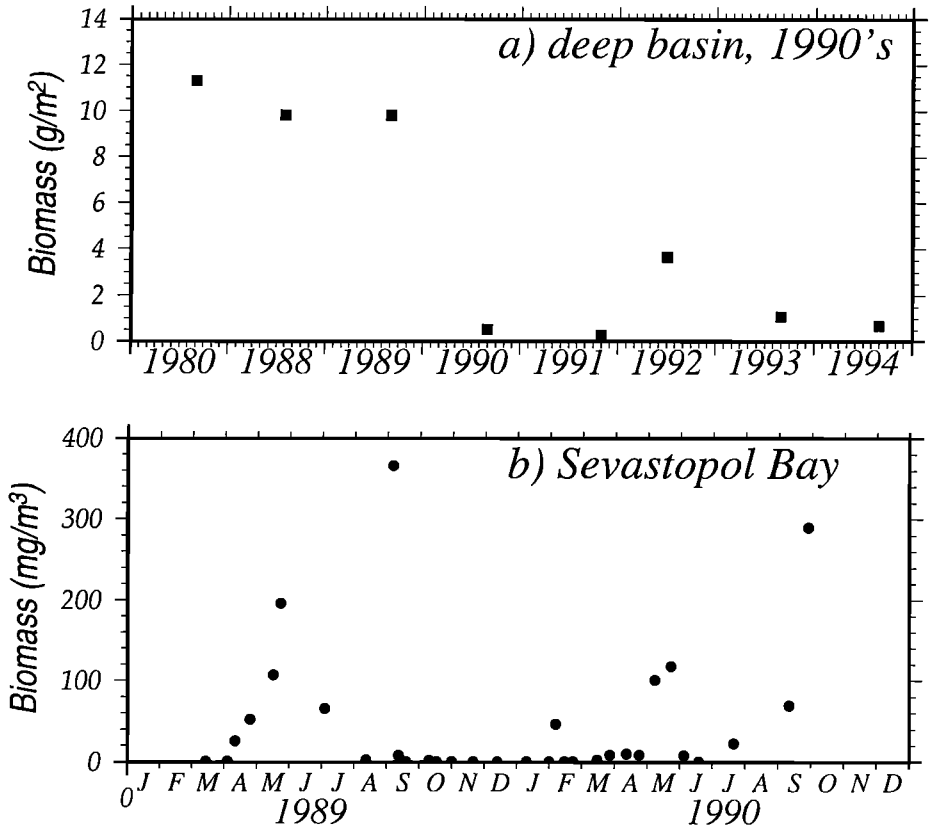


**Figure 11.** *Noctiluca* biomass (a) within the interior basin during the 1980-1994 period (in mg $m^{-3}$) [after *Kovalev et al.*, 1998] and (b) within Sevastopol Bay during 1989-1990 (in g $m^{-2}$). The Sevastopol Bay data were kindly provided by the Institute of Biology of Southern Seas, Sevastopol, Ukraine.

different stages in response to the changing gelatinous carnivore community. The fundamental question we address here is how top-down control by gelatinous predators operates as they reduce mesozooplankton grazing, which may favor increased phytoplankton blooms.

Modeling the gelatinous carnivores is not a straightforward issue and ideally may require implementing population dynamics models involving a series of site specific, empirically based parameterizations for feeding, respiration, reproduction, and mortality characteristics. Such an approach is, however, beyond the scope of the present work. Hence we follow a simplified approach and consider that each of the *Mnemiopsis* or *Aurelia* populations are represented by a single state variable expressed in biomass units. We then mimic their annual biomass cycles by introducing time-dependent growth rate parameterizations. This approach may be justified for our present purpose of not modeling the gelatinous carnivores themselves but investigating their impacts on the other components of the food web.

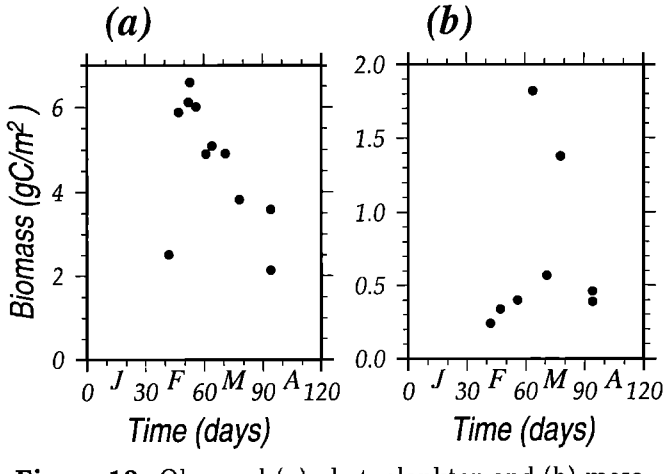


**Figure 12.** Observed (a) phytoplankton and (b) mesozooplankton biomass distributions (in gC $m^{-2}$) during February-April 1991. Each data value represents an average of several measurements within the interior basin.

The pre-*Mnemiopsis* simulation was quite successful in reproducing observations from a set of in situ measurements performed during 1978 at a station off the Caucasian coast of the Black Sea. It was also supported by other independent measurements from different parts of the Black Sea during the late 1970s and early 1980s. The major bloom event takes place during the late winter to early spring season as a consequence of nutrient accumulation in the surface waters at the end of the winter mixing season as soon as the water column receives sufficient solar radiation. Two successive and longer lasting events take place during the spring to early summer and autumn periods.

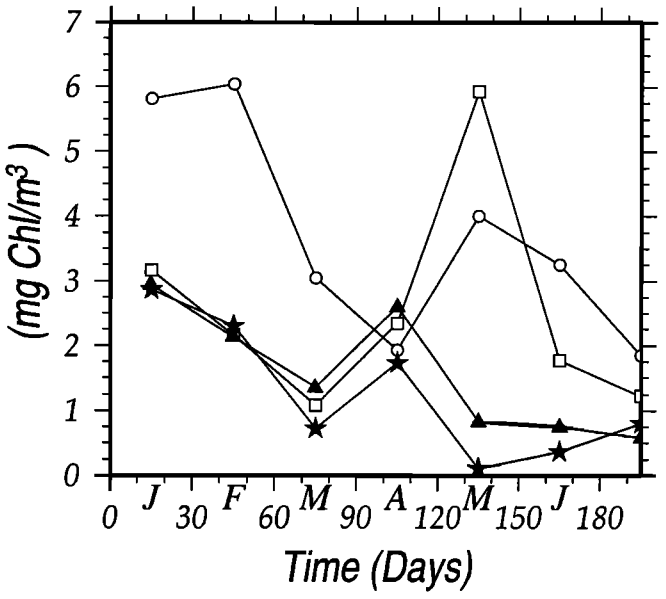


**Figure 13.** The composite monthly mean surface chlorophyll distributions for the January-June period. They are formed by the data collected during 1990-1995 in Bulgarian coastal waters (open circles), the southwestern Turkish shelf (open squares), the wide topographic slope region between the northwestern shelf and western basin interior (solid triangles), and the deep western basin (solid stars) [after *Yilmaz et al.*, 1998].

The early spring phytoplankton bloom is followed first by a mesozooplankton bloom of comparable intensity, which reduces the phytoplankton stock to a relatively low level and then by an *Aurelia* bloom that similarly grazes down the mesozooplankton. The phytoplankton recover and produce a weaker late spring bloom, which triggers a steady increase in *Noctiluca* biomass during the midsummer. As the *Aurelia* population decreases in August, the mesozooplankton first and phytoplankton and *Aurelia* later give rise to successive blooms during September-October period. These blooms were followed by a secondary *Noctiluca* bloom in November.

Introduction of *Mnemiopsis* led to a new type of annual plankton distribution in the ecosystem. The phytoplankton structure was then characterized by three successive and intense bloom periods during winter, spring, and summer. The winter bloom is, in fact, a modified version of the late winter event of the pre-*Mnemiopsis* era. The other two blooms may also be interpreted as the modified forms of late spring to early summer and autumn events reported for the pre-*Mnemiopsis* case, as intensified and shifted ahead by ~2 months.

The winter phytoplankton bloom is a consequence of the particular form of grazing pressure exerted by *Mnemiopsis*, which almost completely depletes the microzooplankton, mesozooplankton, and *Noctiluca* stocks toward the end of autumn season. The lack of grazing on the phytoplankton community then promotes earlier growth starting by the beginning of January. In the previous case of *Aurelia* dominance, on the other hand, the zooplankton community developed following the autumn bloom event prevented early initiation of phytoplankton growth. Winter blooms with that intensity were not reported until the 1990s but were captured during February-March 1990, and 1991 observations [*Yilmaz et al.*, 1998; *Shushkina et al.*, 1998]. These observations therefore provide a certain degree of confidence in the realism of the simulations.

The other interesting feature is that the generation of *Noctiluca* peaks 2 months earlier, as compared with the pre-*Mnemiopsis* period, is supported by the observations. These temporal shifts are related to similar shifts in the phytoplankton blooms.

## Appendix A: Formulation of Bacterioplankton and Nitrogen Cycling

Modeling the temporal and vertical distributions of bacterioplankton is a challenging aspect of Black Sea biogeochemistry since different bacterial populations play different roles in different parts of the water column from the surface to the suboxic/anoxic interface zone. In the present study we simply consider just a single aggregated heterotrophic bacterial group for which the source-sink terms are expressed by

$$\Re(B) = [G_b(\mathrm{DON}) + G_b(D)]\,B - G_s(B)Z_s - G_n(B)Z_n - \mu_s B, \qquad \text{(A1)}$$

where dissolved and particulate organic nitrogen constitute the only food sources. We therefore ignore ammonium uptake by bacterioplankton and assume that their nitrogen requirements are met by organic matter uptake [*Walsh and Dieterle*, 1994; *Baretta-Bekker et al.*, 1995]. Moreover, the stoichiometry of DON versus $NH_4$ uptake cannot be adequately formulated in a nitrogen-only model [*Ducklow*, 1994]. In (A1), bacterivory by microzooplankton and mesozooplankton and excretion of ammonium represent the sink terms. The effect of bacterial mortality is included in the excretion term.

The corresponding source-sink terms for the labile pelagic detritus $D$, dissolved organic nitrogen DON, nitrate $NO_3$, nitrite $NO_2$, and ammonium $NH_4$ are given by

$$\begin{aligned}\Re(D) = {} & (1-\gamma_s)[G_s(P_f) + G_s(P_d) + G_s(B) \\ & + G_s(D)]Z_s + (1-\gamma_l)[G_l(P_f) + G_l(P_d) \\ & + G_l(Z_s) + G_l(Z_n) + G_l(D)]Z_l + (1-\gamma_n) \\ & [G_n(Z_s) + G_n(P_f) + G_n(P_d)]Z_n + (1-\gamma_a) \\ & [G_a(Z_s) + G_a(Z_l)]Z_a + (1-\gamma_m)[G_m(Z_s) \\ & + G_m(Z_l)]Z_m + [\lambda_f {P_f}^2 + \lambda_d {P_d}^2 + \lambda_s Z_s \\ & + \lambda_l Z_l + \lambda_n Z_n + \lambda_a Z_a + \lambda_m Z_m] \\ & - [\gamma_s G_s(D)Z_s + \gamma_l G_l(D)Z_l + \gamma_n G_n(D)Z_n \\ & + G_b(D)B] - \epsilon[f_n(\mathrm{O_2}) + f_d(\mathrm{O_2})]D, \qquad \text{(A2)}\end{aligned}$$

$$\Re(\mathrm{DON}) = \chi\Phi f_p(T)[\sigma_f P_f + \sigma_d P_d] + (1-\kappa)\epsilon[f_n(\mathrm{O_2}) + f_d(\mathrm{O_2})]D - G_b(\mathrm{DON})B, \quad \text{(A3)}$$

$$\Re(\mathrm{NH_4}) = \kappa\epsilon[f_n(\mathrm{O_2}) + f_d(\mathrm{O_2})]D - (\frac{\beta_a}{\beta_t})\Phi f_p(T)[\sigma_f P_f + \sigma_d P_d] + [\mu_s Z_s + \mu_l Z_l + \mu_n Z_n + \mu_a Z_a + \mu_m Z_m + \mu_b B] - k_1 f_n(\mathrm{O_2})\mathrm{NH_4}, \quad \text{(A4)}$$

$$\Re(\mathrm{NO_2}) = k_1 f_n(\mathrm{O_2})\mathrm{NH_4} - k_2 f_n(\mathrm{O_2})\mathrm{NO_2} + k_3 f_d(\mathrm{O_2})\mathrm{NO_3} - k_4 f_d(\mathrm{O_2})\mathrm{NO_2}, \quad \text{(A5)}$$

$$\Re(\mathrm{NO_3}) = k_2 f_n(\mathrm{O_2})\mathrm{NO_2} - k_3 f_d(\mathrm{O_2})\mathrm{NO_3} - (\frac{\beta_n}{\beta_t})\Phi f_p(T)[\sigma_f P_f + \sigma_d P_d]. \quad \text{(A6)}$$

Fecal pellets, constituting the unassimilated part of ingested food (the group of terms inside the first five square brackets in A2) as well as dead phytoplankton and zooplankton (the terms inside the sixth square bracket), are the sources of labile sinking particulate organic matter (detritus). They are recycled in the water column as a result of ingestion by zooplankton (represented by the terms involving $G_s(D)$, $G_l(D)$, and $G_n(D)$), as well as aerobic and anaerobic decomposition (terms inside the last square bracket). The particulate organic material sinks with a single settling velocity $w_d$, which is specified in the form of a Michaelis-Menten-type hyperbolic function with $w_d^*$ representing the maximum sinking velocity and $R_d$ representing the half-saturation constant [see *Oguz et al.*, 2000]. A similar formalism is also adopted for parameterizing diatom sinking. This formulation specifies a linear increase with increasing concentrations and then imposes an asymptotic limit at higher concentrations. Imposing such a limit turns out to be necessary to avoid detritus loss from the bottom boundary of the model and thus to obtain a more realistic nitrogen cycling in the water column within the limitations of a one-dimensional model.

The efficiency of aerobic decomposition occurs at the rate $\epsilon_n f_n(\mathrm{O_2})D$ in the oxygenated part of the water column. The oxygen limitation function $f_n(\mathrm{O_2})$ controlling this process is expressed by a Michaelis-Menten-type hyperbolic function

$$f_n(\mathrm{O_2}) = \frac{\mathrm{O_2}}{\mathrm{O_2} + R_O}, \qquad \mathrm{O_2} \geq 3\mu\mathrm{M}, \quad \text{(A7)}$$

which decreases with decreasing oxygen concentrations and terminates at oxygen concentrations $< 3\ \mu$M. The threshold oxygen value chosen here is consistent with observations [e.g., *Lipschultz et al.*, 1990; *Yakushev and Neretin*, 1997], which report a range of values between 1 and 5 $\mu$M in different oceanic regions.

Where oxygen is depleted lower in the water column, decomposition of particulate material occurs anaerobically by utilizing the nitrate abundant from below the euphotic zone to the base of the suboxic layer. This process is controlled by the limitation function $f_d(\mathrm{O_2})$:

$$f_d(\mathrm{O_2}) = \left[\frac{K_O}{K_O + \mathrm{O_2}}\right], \qquad \mathrm{O_2} < 3\mu\mathrm{M}, \quad \text{(A8)}$$

which provides a maximum rate of anaerobic decomposition at zero oxygen concentration and its gradual decrease as the oxygen concentration increases [*Yakushev and Neretin*, 1997]. When $\mathrm{O_2} \geq 3\mu$M, $f_d(\mathrm{O_2})$ is set to zero. In (A7) and (A8) we take $\mathrm{R}_O$=10 $\mu$M and $\mathrm{K}_O$=2.5 $\mu$M.

In (A3), phytoplankton exudation and a specific fraction of detritus breakdown constitute the two sources of DON to be utilized by bacteria. The rest of detrital breakdown and all the zooplankton excretion are converted directly to ammonium. With this simplified DON cycle we include an additional contribution from zooplankton excretion, which typically amounts to 25% [*Fasham et al.*, 1990].

In the ammonium equation (A4), excretion by the zooplankton groups and bacteria and the fraction of particulate matter ammonified constitute the ammonium sources. The losses are uptake during phytoplankton production and oxidation to nitrite in the aerobic conditions, as the first step of the nitrification process.

Nitrite concentrations in the euphotic zone are always smaller than the other forms of nitrogen [*Codispoti et al.*, 1991; *Basturk et al.*, 1994]. Thus the contribution of nitrite uptake to the phytoplankton production is small as modeled previously by *Oguz et al.* [1998a]. The nitrite equation (A5) involves only terms related to the oxidation-reduction reactions of the nitrification and denitrification processes. The first two terms represent the ammonium to nitrite and nitrite to nitrate oxidation reactions of the nitrification process in oxygenated waters. The last two terms define the denitrification process under oxygen deficient conditions. The third term models nitrate to nitrite reduction, and the fourth term represents nitrite reduction to nitrogen gas. The nitrate equation (A6) consists of a source term due to nitrification (the first term) and loss terms associated with nitrate reduction (the second term) and uptake by phytoplankton (the third term).

**Acknowledgments.** This work is supported in part by the NSF grant OCE-9906656 to T. Oguz and P. Malanotte-Rizzoli and OCE-9908092 to H. W. Ducklow. T. Oguz also acknowledges NATO linkage grant EST.CLG975821, which enabled him to interact with various scientists from other Black Sea countries. It is a contribution to the Black Sea-ODBMS Project sponsored by the NATO Science for Peace Program. We thank the reviewers for their constructive comments.

## References

Aksnes, D. L., and U. Lie, A coupled physical-biological pelagic model of a shallow sill fjord, *Estuarine Coastal Shelf Sci., 31*, 459-486, 1990.

Andersen, V., P. Nival, and R. P. Harris, Modeling of a planktonic ecosystem in an enclosed water column, *J. Mar. Biol. Assoc. U. K., 67*, 407-430, 1990.

Baretta-Bekker, J. G., J. W. Baretta, and E. K. Rasmussen, The microbial food web in the European Regional Seas Ecosystem Model, *Neth. J. Sea Res., 33*, 363-379, 1995.

Basturk, O., C. Saydam, I. Salihoglu, L. V. Eremeeva, S. K. Konovalov, A. Stoyanov, A. Dimitrov, A. Cociasu, L. Dorogan, and M. Altabet, Vertical variations in the principle chemical properties of the Black Sea in the autumn of 1991, *J. Mar. Chem., 45*, 149-165, 1994.

Behrends, G., and G. Schneider, Impact of *Aurelia aurita* medusae (Cnidaria, Scyphozoa) on the standing stock and community composition of mesozooplankton in the Kiel bight (western Baltic Sea), *Mar. Ecol. Prog. Ser., 127*, 39-45, 1995.

Belyaev, V. I., and N. V. Konduforova, Modeling of the shelf ecosystem, *Ecol. Model., 60*, 95-118, 1992.

Bumann, D., and G. Puls, Infestation with larvae of the sea anemone *Edwarsia lineata* affects nutrition and growth of the cteneophore *Mnemiopsis ledyi*, *Parasitology, 113*, 123-128, 1996.

Carpenter, S. R., J. F. Kitchell, and J. R. Hodgson, Cascading trophic interactions and lake productivity, *BioScience, 35*, 634-639, 1985.

Codispoti, L. A., G. E. Friederich, J. W. Murray, and C. M. Sakamoto, Chemical variability in the Black Sea: Implications of continuous vertical profiles that penetrated the oxic/anoxic interface, *Deep Sea Res., Part A, 38*, suppl. 2, S691- S710, 1991.

Cokasar, T., and E. Ozsoy, Comparative analyses and modeling for regional ecosystems of the Black Sea, in *Ecosystem Modeling as a Management Tool for the Black Sea*, vol. 2, *NATO Sci. Partnership Sub-ser.* 2, vol. 47, edited by L. I. Ivanov, and T. Oguz, pp. 323-358, Kluwer Acad., Norwell, Mass., 1998.

Ducklow, H. W., Modeling the microbial foodweb, *Microbial Ecol., 28*, 303-319, 1994.

Eeckhout, D. V., and C. Lancelot, Modeling the functioning of the northwestern Black Sea ecosystem from 1960 to present, in *Sensitivity to Change: Black Sea, Baltic Sea and North Sea, NATO Sci. Partnership Sub-ser.* 2, vol. 27, edited by E. Ozsoy and A. Mikaelyan, pp. 455-469, Kluwer Acad., Norwell, Mass., 1997.

Fasham, M. J. R., H. W. Ducklow, and S. M. McKelvie, A nitrogen-based model of plankton dynamics in the oceanic mixed layer, *J. Mar. Res., 48*, 591-639, 1990.

Fasham, M. J. R., P. W. Boyd, and G. Savidge, Modeling the relative contribution of autotrophs and heterotrophs to carbon flow at a Lagrangian JGOFS station in the Northeast Atlantic: The importance of DOC, *Limnol. Oceanogr., 44*, 80-94, 1999.

Finenko, G. A., G. I. Abolmasova, and Z. A. Romanova, Feeding, respiration, and growth of the ctenophore *Mnemiopsis mccradyi* in relation to grazing conditions, *Russian J. Mar. Bio., Engl. Transl., 21*, 283-287, 1995.

Gargett, A. E., Vertical eddy diffusivity in the ocean interior, *J. Mar. Res., 42*, 359-393, 1984.

Gregg, M. C., and E. Ozsoy, Mixing on the Black Sea shelf north of the Bosphorus, *Geophys. Res. Lett., 26*, 1869-1872, 1999.

Gregoire, M., J. M. Beckers, J. C. J. Nihoul, and E. Stanev, Reconnaissance of the main Black Sea's ecohydrodynamics by means of a 3D interdisciplinary model, *J. Mar. Syst., 16*, 85-106, 1998.

Gucu, A. C., Role of fishing in the Black Sea ecosystem, in *Sensitivity to Change: Black Sea, Baltic Sea and North Sea, NATO Sci. Partnership Sub-ser.* 2, vol. 27, edited by E. Ozsoy and A. Mikaelyan, pp. 149-162, Kluwer Acad., Norwell, Mass., 1997.

Hairston, N. G., F. E. Smith, and L. B. Slobodkin, Community structure, population control and competition, *Am. Nat.*, 94, 421-425, 1960.

Hamner, W. M., and R. M. Jenssen, Growth, degrowth, and irreversible cell differentiation in *Aurelia aurita*, *Am. Zool., 14*, 833-849, 1974.

Ishii, H., and U. Bamstedt, Food regulation of growth and maturation in a natural population of *Aurelia aurita*, *J. Plankton Res., 20*, 805-816, 1998.

Ivanov, L. I., and T. Oguz, *Ecosystem Modeling as a Management Tool for the Black Sea*, vol. 1, *NATO Sci. Partnership Sub-ser.* 2, vol. 47, Kluwer Acad., Norwell, Mass., 1998.

Ivanov, L. I., and T. Oguz, *Ecosystem Modeling as a Management Tool for the Black Sea*, vol. 2, *NATO Sci. Partnership Sub-ser.* 2, vol. 47, Kluwer Acad., Norwell, Mass., 1998.

Khoroshilov, V. S., Seasonal dynamics of the Black Sea population of the ctenophore *Mnemiopsis leidyi*, *Oceanology, Engl. Transl., 33*, 482-485, 1994.

Kideys, A. E., A. V. Kovalev, G. Shulman, A. Gordina, and F. Bingel, A review of zooplankton investigations of the Black Sea over the last decade, *J. Mar. Syst., 24*, 355-371, 2000.

Kovalev, A. V., U. Nierman, V. V. Melnikov, V. Belokopytov, Z. Uysal, A. E. Kideys, M. Unsal, and D. Altukhov, Longterm changes in the Black Sea zooplankton: The role of natural and anthropogenic factors, in *Ecosystem Modeling as a Management Tool for the Black Sea*, vol. 1, *NATO Sci. Partnership Sub-ser.* 2, vol. 47, edited by L. I. Ivanov, and T. Oguz, pp. 221-234, Kluwer Acad., Norwell, Mass., 1998.

Kovalev, A. V., and S. A. Piontkovski, Interannual changes in the biomass of the Black Sea gelatinous zooplankton, *J. Plankton Res., 20*, 1377-1385, 1998.

Kremer, P., Excretion and body composition of the ctenophore *Mnemiopsis leidyi* (A. Agassiz): Comparisons and consequences, in *10th European Symposium on Marine Biology*, vol. 2, edited by G. Persoone and E. Jaspers, pp. 351-362, Universal, Weeteren, Belgium, 1976a.

Kremer, P., The population dynamics and ecological energetics of a pulsed zooplankton predator, the ctenophore *Mnemiopsis leidyi*, in *Estuarine Processes*, vol. 1, edited by G. Wiley, G., pp. 197-215, Academic, San Diego, Calif., 1976b.

Kremer, P., Respiration and excretion by ctenophore *Mnemiopsis leidyi*, *Mar. Biol., 44*, 43-50, 1977.

Kremer, P., Patterns of abundance for Mnemiopsis in US coastal waters: A comparative overview, *ICES J. Mar. Sci., 51*, 347-354, 1994.

Kremer, J. N., and S. W. Nixon, *A coastal Marine Ecosystem, Simulation and Analysis*, 217 pp., Springer-Verlag, New York, 1978.

Larson, R. J., Water content, organic content, and carbon and nitrogen composition of medusae from the northeast Pacific, *J. Exp. Mar. Biol. Ecol., 99*, 107-120, 1986.

Lebedeva, L. P., and E. A. Shushkina, Evaluation of population characteristics of the medusae *Aurelia aurita* in the Black Sea, *Oceanology, Engl. Transl., 31*, 314-319, 1991.

Lebedeva, L. P., and E. A. Shushkina, Modeling the effect of *Mnemiopsis* on the Black Sea plankton community, *Oceanology, Engl. Transl., 34*, 72-80, 1994.

Lipschultz, F., S. C. Wofsy, B. B. Ward, L. A. Codispoti, G. Friedrich, and J. W. Elkins, Bacterial transformations of inorganic nitrogen in the oxygen-deficient waters of the eastern tropical South Pacific Ocean, *Deep Sea Res., Part I, 37*, 1513-1541, 1990.

Lucas, C. H., and J. A. Williams, Population dynamics of scyphomedusa *Aurelia aurita* in Southampton water, *J. Plankton Res., 16*, 879-895, 1994.

Mee, L. D., The Black Sea in crisis: A need for concerted international action, *Ambio, 21*, 278-286, 1992.

Micheli, F., Eutrophication, fisheries and consumer-resource

dynamics in marine pelagic ecosystems, *Science, 285*, 1396- 1398, 1999.

Mikaelyan, A.S., Long-term variability of phytoplankton communities in open Black Sea in relation to environmental changes, in *Sensitivity to change: Black Sea, Baltic Sea and North Sea, NATO Sci. Partnership Sub-ser., 2*, vol. 27, edited by E. Ozsoy and A. Mikaelyan, pp. 105-116, Kluwer Acad., Norwell, Mass., 1997.

Mills, C. E., Natural mortality in NE Pacific coastal hydromedusae: grazing predation, wound healing and senescence, *Bull. Mar. Sci., 53*, 194-203, 1993.

Minkina, N. I., and E. V. Pavlova, Diurnal changes of the respiration rate in the comb jelly *Mnemiopsis leidyi* in the Black Sea, *Oceanology, Engl. Transl., 35*, 222-225, 1995.

Moller, H., Population dynamics of *Aurelia aurita* medusae in Kiel Bight, Germany (FRG), *Mar. Biol., 60*, 123-128, 1980.

Moller, H., Reduction of a larval herring population by jellyfish predator, *Science, 224*, 621-622, 1984.

Moncheva, S., and A. Krastev, Some aspects of phytoplankton long-term alterations off Bulgarian Black Sea shelf, in *Sensitivity to change: Black Sea, Baltic Sea and North Sea, NATO Sci. Partnership Sub-ser.* 2, vol. 27, edited by E. Ozsoy and A. Mikaelyan, pp. 79-94, Kluwer Acad., Norwell, Mass., 1997.

Mutlu, E., Distribution and abundance of ctenophores and their zooplankton food in the Black Sea, II, *Mnemiopsis leidyi, Mar. Biol., 135*, 603-613, 1999.

Mutlu, E., F. Bingel, A. C. Gucu, V. V. Melnikov, U. Niermann, N. A. Ostr, and V. E. Zaika, Distribution of the new insader *Mnemiopsis sp.* and the resident *Aurelia aurita* and *Pleurobrachia pileus* populations in the Black Sea in the years 1991-1993, *ICES J. Mar. Sci., 51*, 407-421, 1994.

Nemazie, D. A., J. E. Purcell, and P. M. Glibert, Ammonium excretion by gelatinous zooplankton and their contribution to the ammonium requirements of microplankton in Chesapeake Bay, *Mar. Biol., 116*, 451-458, 1993.

Nezlin, N. P., A. G. Kostianoy, and M. Gregoire, Patterns of seasonal and interannual changes of surface chlorophyll concentration in the Black Sea revealed from the remote sensed data, *Remote Sens. Environ., 69*, 43-55, 1999.

Oguz, T., H. Ducklow, P. Malanotte-Rizzoli, S. Tugrul, N. Nezlin, and U. Unluata, Simulation of annual plankton productivity cycle in the Black Sea by a one-dimensional physical-biological model, J. Geophys. Res., 101, 16585-16599, 1996. Simulation of annual plankton productivity cycle in the Black Sea by a one-dimensional physical-biological model, *J. Geophys. Res., 101*, 16,585-16,599, 1996.

Oguz, T., H. Ducklow, E. A. Shuskina, P. Malanotte-Rizzoli, S. Tugrul, and L. P. Lebedeva, Simulation of upper layer biogeochemical structure in the Black Sea, in *Ecosystem Modeling as a Management Tool for the Black Sea*, vol. 2, *NATO Sci. Partnership Sub-ser.* 2, vol. 47, edited by L. I. Ivanov, and T. Oguz, pp. 257-300, Kluwer Acad., Norwell, Mass., 1998a.

Oguz, T., H. Ducklow, P. Malanotte-Rizzoli, and J. W. Murray, Simulations of the Black Sea pelagic ecosystem by one dimensional vertically resolved physical-biochemical models, *Fish. Oceanogr., 7*, 300-304, 1998b.

Oguz, T., H. Ducklow, P. Malanotte-Rizzoli, J. W. Murray V.I. Vedernikov, and U. Unluata, A physical-biochemical model of plankton productivity and nitrogen cycling in the Black Sea, *Deep Sea Res., part I, 46*, 597-636, 1999.

Oguz, T., H. Ducklow, and P. Malanotte-Rizzoli, Modeling distinct vertical biogeochemical structure of the Black Sea: Dynamical coupling of the oxic, suboxic and anoxic layers, *Global Biogeochem. Cycles*, in press, 2000.

Oguz, T., J. W. Murray, and A. E. Callahan, Modeling redox cycling across the suboxic-anoxic interface zone in the Black Sea, *Deep Sea Res., Part I, 48*, 761-787, 2001.

Olesen, N. J., K. Frandsen, and H. U. Riisgard, Population dynamics, growth and energetics of jellyfish *Aurelia aurita* in a shallow fjors, *Mar. Ecology Prog. Series, 105*, 9-18, 1994.

Olesen, N. J., J. E. Purcell, and D. K. Stoecker, Feeding and growth by ephyrae of scyphomedusae *Chrysaora quinquecirrha, Mar. Ecol. Prog. Ser., 137*, 149-159, 1996.

Ozsoy, E., and A. S. Mikaelyan, *Sensitivity to Change: Black Sea, Baltic Sea and North Sea, NATO Sci. Partnership Sub-ser.* 2, vol. 27, 469 pp., Kluwer Acad., Norwell, Mass., 1997.

Purcell, J. E., Quantification of *Mnemiopsis leidyi* (Ctenophora, Lobata) from formalin-preserved plankton samples, *Mar. Ecol. Prog. Ser., 45*, 197-200, 1988.

Purcell, J. E., Predation by *Aequorea victoria* on other species of potentially competing pelagic hydrozoans, *Mar. Ecol. Prog. Ser., 72*, 255-260, 1991.

Purcell, J. E., and J. H. Cowan Jr., Predation by the scyphomedusan *Chrysaora quinquecirrha* on *Mnemiopsis leidyi, Mar. Ecol. Prog. Ser., 128*, 63-70, 1995.

Purcell, J. E., and P. Kremer, Feeding and metabolism of the siphonophore *Sphaeronectes gracilis, J. Plankton Res., 5*, 95-106, 1983.

Purcell, J. E., D. A. Nemazie, S. E. Dorsey, E. D. Houde, and J. C. Gamble, Predation mortality of bay anchovy (*Anchoa mitchilli*) eggs and larvae due to scyphomedusae and ctenophores in Chesapeake Bay, *Mar. Ecol. Prog. Ser., 114*, 47-58, 1994a.

Purcell, J. E., J. R. White, and M. R. Roman, Predation by gelatinous zooplankton and resource limitation as potential controls of *Acartia tonsa* copepod populations in Chesapeake Bay, *Limnol. Oceanogr., 39*, 263-278, 1994b.

Rass, T. S., Changes in the fish resources of the Black Sea, *Oceanology, Engl. Transl., 32*, 197-203, 1992.

Reeve, M. R., M. A. Syms, and P. Kremer, Growth dynamics of a ctenophore (*Mnemiopsis*) in relation to variable food supply I. Carbon biomass, feeding, egg production, growth, and assimilation efficiency, *J. Plankton Res., 11*, 535-552, 1992.

Schneider, G., and G. Behrends, Population dynamics and the trophic role of *Aurelia aurita* medusae in the Kiel Bight and western Baltic, *ICES J. Mar. Sci., 51*, 359-367, 1989.

Shiganova, T. A., Invasion of the Black Sea by the ctenophore *Mnemiopsis leidyi* and recent changes in pelagic community structure, *Fish. Oceanogr., 7*, 305-310, 1998.

Shiganova, T. A., A. E. Kideys, A. C. Gucu, U. Niermann, and V. S. Khoroshilov, Changes in species diversity and abundance of the main components of the Black Sea plelagic community during the last decade, in *Ecosystem Modeling as a Management Tool for the Black Sea*, vol. 1, *NATO Sci. Partnership Sub-ser.* 2, vol. 47, edited by L. I. Ivanov, and T. Oguz, pp. 171-188, Kluwer Acad., Norwell, Mass., 1998.

Shushkina, E. A., and E. I. Musayeva, The role of jellyfish in the energy system of the Black Sea plankton communities, *Oceanology, Engl. Transl., 23*, 92-96, 1983.

Shushkina, E. A., and E. I. Musayeva, Structure of pelagic community of the Black Sea epipelagic zone and its variation caused by invasion of a new ctenophore species, *Oceanology, Engl. Transl., 30*, 225-228, 1990.

Shushkina, E. A., and M. E. Vinogradov, Long-term changes in the biomass of plankton in open areas of the Black Sea, *Oceanology, Engl. Transl., 31*, 716-721, 1991.

Shushkina, E. A., Y. I. Sorokin, L. P. Lebedeva, A. F. Pasternak, and E. E. Koshevskaya, Production and destruction characteristics of plankton community in the northeastern part of the Black Sea during 1978 (in Rus-

sian), in *Seasonal variations of Black Sea plankton*, edited by Y. I. Sorokin and V. I. Vedernikov, pp. 178-200, Nauka, Moscow, 1983.

Shushkina, E. A., M. E. Vinogradov, L. P. Lebedeva, T. Oguz, N. P. Nezlin, V. Yu. Dyakonov, and L. L. Anokhina, Studies of structural parameters of planktonic communities of the open part of the Black Sea relevant to ecosystem modeling, in *Ecosystem Modeling as a Management Tool for the Black Sea*, vol. 1, *NATO Sci. Partnership Subser.* 2, vol. 47, edited by L. I. Ivanov, and T. Oguz, pp. 311-326, Kluwer Acad., Norwell, Mass., 1998.

Sorokin, Y. I., The Black Sea, in *Ecosystems of the World*, vol. 26, *Estuaries and Enclosed Seas*, edited by B. H. Ketchum, pp. 253-292, Elsevier Sci., New York, 1983.

Staneva, J., E. Stanev, and T. Oguz, On the sensitivity of the planktonic cycle to physical forcing: Model study on the time variability of the Black Sea ecological system, in *Ecosystem Modeling as a Management Tool for the Black Sea*, vol. 2, *NATO Sci. Partnership Sub-ser.* 2, vol. 47, edited by L. I. Ivanov, and T. Oguz, pp. 301-322, Kluwer Acad., Norwell, Mass., 1998.

Stoecker, D. K, A. E. Michaels, and L. H. Davis, Grazing by the jellyfish, *Aurelia aurita*, on microzooplankton, *J. Plankton Res., 9*, 901-915, 1987.

Strong, D. R., Are trophic cascades all wet? Differentiation and donor-control in speciose ecosystems, *Ecology, 73*, 747-754, 1992.

Sullivan, B. K., J. R. Garcia, and G. Klein-Macphee, Prey selection by the scyphomedusan predator *Aurelia aurita*, *Mar. Biol., 121*, 335-341, 1994.

Tugrul, S., O. Basturk, C. Saydam, and A. Yilmaz, The use of water density values as a label of chemical depth in the Black Sea, *Nature, 359*, 137-139, 1992.

Van der Veer, H. W., and W. Oorthuysen, Abundance, growth and food demand of the scyphomedusa *Aurelia aurita* in the western Wadden Sea, *Neth. J. Sea Res., 19*, 38-44, 1985.

Varela, R. A., A. Cruzado, and J.E. Gabaldon, Modeling primary production in the North Sea using European Regional Seas Ecosystem Model, *Neth. J. Sea Res., 33*, 337-361, 1995.

Vedernikov, V. I., and A. B. Demidov, Primary production and Chlorophyll in deep regions of the Black Sea, *Oceanology, Engl. Transl., 33*, 193-199, 1993.

Vedernikov, V. I., and A. B. Demidov, Vertical distribution of primary production and chlorophyll during different seasons in deep regions of the Black Sea, *Oceanology, Engl. Transl., 37*, 376-384, 1997.

Verity, P. G., and V. Smetacek, Organism life cycles, predation, and the structure of marine pelagic ecosystems, *Mar. Ecol. Prog. Ser., 130*, 277-293, 1996.

Vinogradov, M. E., and E. A. Shushkina, Temporal changes in community structure in the open Black Sea, *Oceanology, Engl. Transl., 32*, 485-491, 1992.

Vinogradov, M. E., E. A. Shushkina, Y. V. Bulgakova, and I. I. Serobaba, Consumption of zooplankton by the comb jelly *Mnemiopsis leidyi* and pelagic fishes in the Black Sea, *Oceanology, Engl. Transl., 35*, 523-527, 1996.

Volovik, S. Y., S. P. Volovik, and Z. A. Myrzoyan, Modeling of the Mnemiopsis sp. population in the Azov Sea, *ICES J. Mar. Sci., 52*, 735-746, 1995.

Walsh, J. J., and D. A. Dieterle, $CO_2$ cycling in the coastal ocean, I, A numerical analysis of the southern Bering Sea with applications to the Chukchi Sea and the northern Gulf of Mexico, *Prog. Oceanogr., 34*, 335-392, 1994.

Yakushev, E. V., and L. N. Neretin, One dimensional modeling of nitrogen and sulfur cycles in the aphotic zone of the Black and Arabian Seas, *Global Biogeochem. Cycles, 11*, 401-414, 1997.

Yilmaz, A., O. A. Yunev, V. I. Vedernikov, S. Moncheva, A. S. Bologa, A. Cociasu, and D. Ediger, Unusual temporal variations in the spatial distribution of chlorophyll *a* in the Black Sea during 1990-1996, in *Ecosystem Modeling as a Management Tool for the Black Sea*, vol. 1, *NATO Sci. Partnership Sub-ser.* 2, vol. 47, edited by L. I. Ivanov, and T. Oguz, pp. 105-120, Kluwer Acad., Norwell, Mass., 1998.

Zaitsev, Y., and V. Mamaev, *Marine Biological Diversity in the Black Sea: A Study of Change and Decline*, 208 pp., Global Environ. Facil., Black Sea Environ. Prog., New York, 1997.

Hugh W. Ducklow, Virginia Institute of Marine Sciences, College of William and Mary, P.O. Box 1346, Gloucester Point, VA 23062.(duck@vims.edu)

Paola Malanotte-Rizzoli Department of Earth, Atmospheric and Planetary Sciences, Massachusettes Institute of Technology, Cambridge, MA 02139. (rizzoli@mit.edu)

Temel Oguz, Institute of Marine Sciences, Middle East Technical University, Erdemli, P.O. Box 28, 33731, Icel, Turkey. (oguz@ims.metu.edu.tr)

Jennifer E. Purcell, Center for Environmental Science, Horn Point Environmental Laboratory, University of Maryland, Box 775, Cambridge, MD21613. (purcell@hpl.umces.edu)

(Received September 21, 1999; revised June 16, 1999; accepted August 11, 1999.)